**Short Title:** Lipid complement of *Arabidopsis* leaf mitochondria

# Defining the lipidome of Arabidopsis leaf mitochondria: Specific lipid complement and lipid biosynthesis capacity

Yi-Tse Liu[1,†], Jennifer Senkler[2,†], Cornelia Herrfurth[1,3], Hans-Peter Braun[2,*], Ivo Feussner[1,3,4,*]

[1]University of Goettingen, Albrecht-von-Haller-Institute for Plant Sciences, Department of Plant Biochemistry, 37077 Goettingen, Germany. [2]Leibniz Universität Hannover, Institute of Plant Genetics, Department of Plant Proteomics, 30419 Hannover, Germany. [3]University of Goettingen, Goettingen Center for Molecular Biosciences (GZMB), Service Unit for Metabolomics and Lipidomics, 37077 Goettingen, Germany. [4]University of Goettingen, Goettingen Center for Molecular Biosciences (GZMB), Department of Plant Biochemistry, 37077 Goettingen, Germany

***Authors for correspondence:** Hans-Peter Braun, Herrenhäuser Str. 2, 30419 Hannover, Germany; Fax. +49 511 76214351; Email: braun@genetik.uni-hannover.de; Ivo Feussner, Justus-von-Liebig-Weg 11, 37077 Goettingen, Germany; Fax: +49-551-39-25749; Email: ifeussn@uni-goettingen.de

†These authors contributed equally to this work.

The authors responsible for distribution of materials integral to the findings presented in this article in accordance with the policy described in the Instructions for Authors (https://academic.oup.com/plphys/pages/General-Instructions) are Hans-Peter Braun, braun@genetik.uni-hannover.de and Ivo Feussner, ifeussn@uni-goettingen.de.

**Author contributions:** YL performed experiments including lipid analysis and pathway construction; JS performed proteomic analysis. YL, JS, CH, HB and IF analyzed the data. YL wrote

the first draft of the manuscript. CH, HB and IF edited the manuscript. HB and IF designed and supervised the study. IF agrees to serve as the author responsible for contact and ensures communication.

**Competing interests:** Authors declare no competing interest.

**Key words:** *Arabidopsis thaliana*, lipidome, mitochondrium, proteome, respiration

**One sentence summary:** The lipid landscape of plant mitochondria suggests that they are capable in generating several phospholipid classes with the assistant of membrane contact site-localized proteins.

## Summary

Mitochondria are often considered the power stations of the cell, playing critical roles in various biological processes such as cellular respiration, photosynthesis, stress responses and programmed cell death. To maintain the structural and functional integrities of mitochondria, it is crucial to achieve a defined membrane lipid composition between different lipid classes wherein specific proportions of individual lipid species are present. Although mitochondria are capable of self-synthesizing a few lipid classes, many phospholipids are synthesized in the endoplasmic reticulum and transferred to mitochondria via membrane contact sites, as mitochondria are excluded from the vesicular transportation pathway. However, knowledge on the capability of lipid biosynthesis in mitochondria and the precise mechanism of maintaining the homeostasis of mitochondrial lipids is still scarce. Here we describe the lipidome of mitochondria isolated from *Arabidopsis* leaves, including the molecular species of glycerolipids, sphingolipids and sterols to depict the lipid landscape of mitochondrial membranes. In addition, we define proteins involved in lipid metabolism by proteomic analysis and compare our data with mitochondria from cell cultures since they still serve as model system. Proteins putatively localized to the membrane contact sites are proposed based on the proteomic results and online databases. Collectively, our results suggest that leaf mitochondria are capable - with the assistance of membrane contact site-localised proteins - of generating several lipid classes including phosphatidylethanolamines, cardiolipins, diacylgalactosylglycerols and free sterols. We

55 anticipate our work to be a foundation to further investigate the functional roles of lipids and
56 their involvement in biochemical reactions in plant mitochondria.

57

58

59 **Introduction**

60 Mitochondria are considered as semiautonomous organelles. According to a widely accepted
61 hypothesis, they descend from proteobacteria that have been engulfed to form an eukaryotic
62 cell. The two involved cells established an endosymbiosis (Gray et al., 1999). Mitochondria play
63 crucial roles in various cellular processes, including ATP generation, metabolite biosynthesis,
64 stress responses like phosphate starvation and initiation of programmed cell death (Jacoby et al.,
65 2012; Michaud et al., 2016). The mitochondria of plant cells even have extended functions,
66 many of which are related to photosynthesis (Braun, 2020). Mitochondria are enclosed by two
67 membranes, the outer (OM) and the inner (IM) mitochondrial membranes, that both require
68 defined protein and lipid compositions to maintain their functional integrity (Horvath and Daum,
69 2013; Michaud et al., 2017). The majority of the mitochondrial proteins is encoded by the
70 nuclear genome, synthesized in the cytoplasm and post-translationally imported into the
71 organelle. At the same time, a few proteins are encoded by the mitochondrial genome and
72 synthesized within the organelle. Recent studies have broadened the knowledge of protein and
73 lipid import in mitochondria, to the OM, the intermembrane space, the IM and the matrix
74 (Michaud et al., 2017).

75 Biological membranes are composed of a wide variety of lipid classes and molecular species.
76 According to the backbones of the lipid molecules, they are classified into three main lipid
77 categories – glycerolipids, sphingolipids and sterols. To delineate the molecular species in this
78 study, we later use the taxonomy containing two colon-separated units for the numbers of
79 carbons and double bonds in the fatty acyl moiety, and an additional unit after a semicolon for
80 the number of hydroxyl groups (when present) (Liebisch et al., 2020). Plant mitochondrial
81 membranes contain high amounts of glycerophospholipids, such as phosphatidylcholine (PC)
82 and phosphatidylethanolamine (PE), but contain less than 2 % of sterols (Moreau et al., 1974;
83 Bligny and Douce, 1980). Sphingolipids have so far not been detected in mitochondrial

84 membranes form plants. Most of these lipids are produced in the ER and are sorted to
85 mitochondria and other organelles afterwards. Nevertheless, mitochondria have also their own
86 capacity to generate some specific lipid classes. For instance, cardiolipin (CL) is synthesized in
87 the IM and is present exclusively in mitochondria (Douce et al., 1972; Babiychuk et al., 2003). CL
88 plays an essential role establishing the cristae of the IM and in maintaining the mitochondrial
89 ultrastructure. CL is formed through the condensation of phosphatidylglycerol (PG) and
90 diacylglycerol (DAG) and finally consists of four acyl chains. The inner envelope of the plastid is
91 the major site for generating PG molecules (Müller and Frentzen, 2001). However, enzymes
92 involved in PG biosynthesis are identified in mitochondria as well, suggesting that mitochondria
93 are capable of self-synthesizing PG and thus CL (Babiychuk et al., 2003). In plants, the PG
94 synthesizing enzymes, phosphatidylglycerolphosphate (PGP) synthase and PGP phosphatase
95 (PGPP), are associated with mitochondria, and plastids; whereas CL synthase (CLS) localizes
96 exclusively in the IM (Xu et al., 2002; Katayama et al., 2004). Notably, although mitochondrial
97 lipid biosynthesis is not the major lipid source in plant cells, it is critical for certain organisms. In
98 yeast, mitochondria are the major supplier of PE (Horvath and Daum, 2013). They generate PE
99 from phosphatidylserine (PS) by phosphatidylserine decarboxylase (PSD). In *Arabidopsis*, three
100 PSD enzymes have been identified and PSD1 localizes in mitochondria, providing PE molecules *in*
101 *situ* (Nerlich et al., 2007). Alternatively, some PS molecules are converted from PE through the
102 base-exchange pathway that substitutes the head groups of PE with serine molecules by PS
103 synthase1, PSS1 (Yamaoka et al., 2011). While knowing mitochondria are capable of synthesizing
104 PG, CL, PS and PE, its competence toward other lipid classes is still poorly understood (Li-Beisson
105 et al., 2013).

106 Lipid trafficking between ER, mitochondria and plastids is essential for mitochondrial membrane
107 biogenesis (Horvath and Daum, 2013; Michaud et al., 2017). Based on studies in yeast and
108 mammals, glycerophospholipid biosynthesis takes place at a distinct membrane stretch of the
109 ER, the mitochondria-associated membrane (MAM), wherein both ER and mitochondrial
110 proteins have been identified (Vance, 1990). Elevated activities of PE, PC and PS synthesizing
111 enzymes have been detected in purified yeast MAM. Moreover, this distinct membrane domain
112 seems to occur ubiquitously among plants and animal cells, suggesting its critical role during
113 evolution and in mediating lipid transfer between ER and mitochondria (Morré et al., 1971;

114 Staehelin, 1997; Achleitner et al., 1999; Michaud et al., 2016). Although mitochondria and
115 plastids work closely together in numerous pathways in plants, the lipid transport mechanism
116 between these two organelles is largely unknown. Nevertheless, a few studies have suggested
117 the relevance of lipid trafficking between these two organelles for survival, especially under
118 environmental stresses. During phosphate starvation, higher numbers of mitochondria – plastid
119 junctions are established (Jouhet et al., 2004). At the same time, drastic lipid remodeling of
120 mitochondria, plastids and plasma membrane arises. PC and PE are degraded to release the
121 phosphate residues for essential biological processes and the remaining molecules are recycled
122 to generate the typical plastidial glyceroglycolipid, digalactosyldiacylglycerol (DGDG). This
123 coincides with increased levels of CL in mitochondria isolated from *Arabidopsis* suspension cells
124 and calli (Michaud et al., 2017). In *Arabidopsis*, the protein complex involved in lipid trafficking
125 and tethering of the two mitochondrial membranes, the mitochondrial transmembrane
126 lipoprotein (MTL) complex, has been identified recently (Michaud et al., 2016). MTL is composed
127 of more than 200 subunits and it has been demonstrated that MTL promotes the translocation
128 of PE from IM to OM and the import of DGDG from plastids to mitochondria during phosphate
129 starvation. Furthermore, mutation of a newly identified MTL subunit, digalactosyldiacylglycerol
130 synthase suppressor 1 (DGS1), leads to alteration of plastidial and mitochondrial lipid
131 composition and deficiency in mitochondrial biogenesis (Li et al., 2019). The characterization of
132 the MTL complex provides an initial insight in understanding the mechanism of lipid trafficking
133 between mitochondria and plastids.

134 In this study, we aimed to characterize the lipid metabolism of *Arabidopsis* leaf mitochondria in
135 depth and to compare these data with published and own data from suspension cell cultures
136 since they serve as model system. Therefore, we conducted an in-depth lipidomic analysis,
137 providing the molecular species information of all lipid categories including glycerolipids,
138 sphingolipids and sterols to illustrate the lipid landscape of mitochondria in *Arabidopsis* leaves.
139 In combination with a proteomic approach, we intended to specify the capacity of lipid
140 biosynthesis and modification in plant mitochondria, defining lipid species and classes that may
141 be generated by mitochondria. We additionally propose putative membrane contact site-
142 localizing proteins and their roles in interorganelle communication. Our results suggest that leaf
143 mitochondria possess a defined lipid composition wherein specific lipid molecular species

144 appear. In addition, lipid trafficking between mitochondria, ER and plastids via membrane
145 contact sites provides assistance in maintaining the homeostasis of the lipid composition in
146 mitochondria.

147 **Results**

148 **Purity of mitochondrial fractions**

149 A combinatorial approach by lipidomics, proteomics and mining of online databases was applied
150 to investigate the lipid composition as well as the capacity of lipid metabolism of *Arabidopsis*
151 leaf mitochondria. Mitochondria were isolated from three independent experiments by
152 differential centrifugation combined with Percoll density gradient centrifugation. To ensure and
153 evaluate the purity of the mitochondrial fractions, all samples were investigated by two-
154 dimensional (2D) blue native (BN)/SDS PAGE and by shotgun proteome analyses. Our
155 mitochondrial fractions proved to be of high purity. The two photosystems were not detectable
156 on our 2D gels. Only trace amounts of the large subunit from Rubisco, the most abundant
157 protein in leaves, were visible in the leaf mitochondrial fractions (L-mito) on BN/SDS gels, and
158 the small subunit of Rubisco was barely visible (Fig. 1A, Supplemental Fig. S1). Since most of the
159 work on plant mitochondria was performed with suspension cell cultures so far, we isolated
160 mitochondria from dark-grown *Arabidopsis* cell culture (C-mito) for comparison. They were
161 investigated by the same procedure and used as an established control for contamination from
162 chloroplasts. The L-mito and C-mito fractions were highly similar on BN/SDS PAGE (Fig. 1,
163 Supplemental Fig. S1). In addition, the purity of the mitochondrial fractions was investigated by
164 label-free quantitative shotgun proteomics. Building on the proteome data (Supplemental Tab.
165 S1), the proportion of mitochondria-localized proteins was calculated to be in the range of 87 to
166 94 % (Fig. 1B, Supplemental Fig. S2). These results indicate that the mitochondrial fractions are
167 of high purity.

168

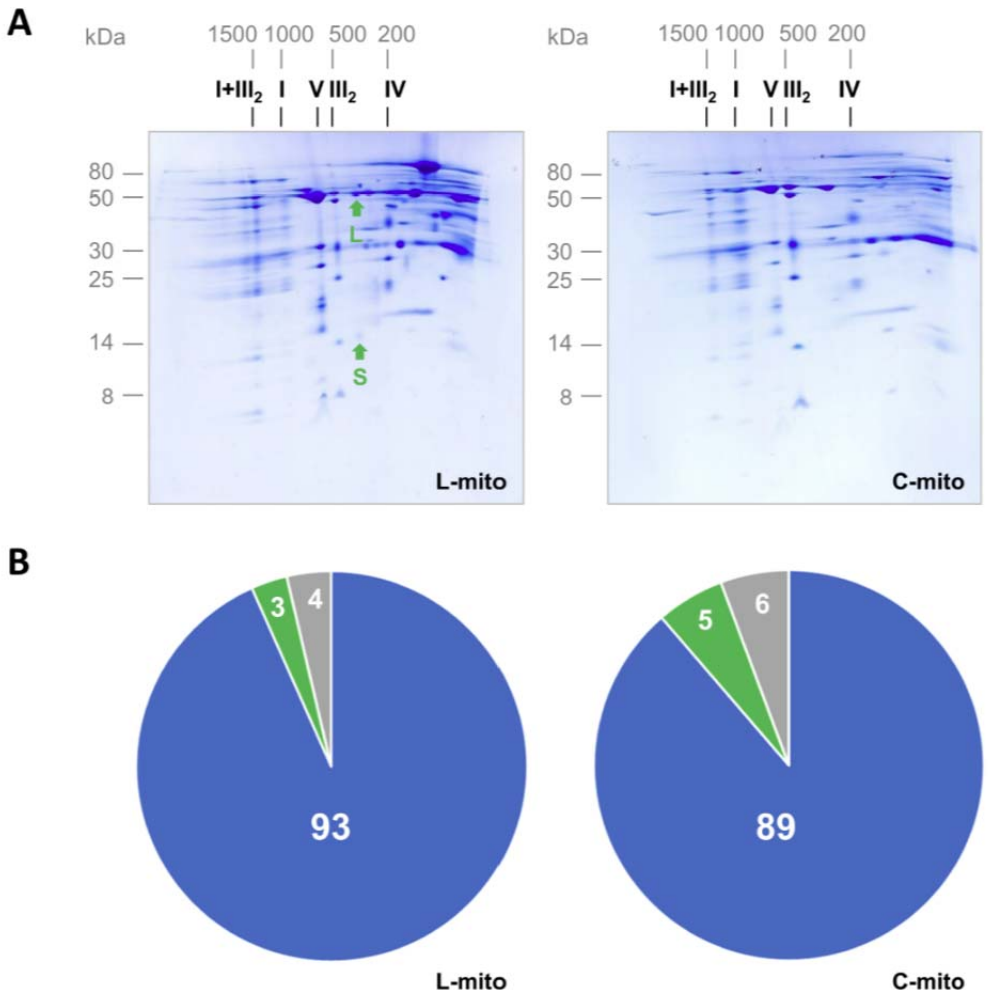


**Figure 1**. Purity of mitochondrial fractions. The purity of mitochondrial fractions was determined by 2D blue native / SDS PAGE **(A)** and by summed-up peptide intensities of subcellular compartments based on protein assignments as given by the Subcellular localization database for Arabidopsis proteins (SUBAcon; www.suba.live) **(B)**.

**A**: Mitochondria were isolated from *Arabidopsis* leaves (L-mito) and cell cultures (C-mito). Proteins were separated by 2D Blue native PAGE and Coommassie-stained. Numbers on top and to the left of the 2D gels refer to the masses of standard protein complexes / proteins (in kDa), the roman numbers above the gels to the identity of OXPHOS complexes. I+$III_2$: supercomplex consisting of complex I and dimeric complex III; I: complex I; V: complex V; $III_2$: dimeric complex III; IV: complex IV. The small (S; 14.5 kDa) and the large (L; 53.5 kDa) subunit of Rubisco are indicated by green arrows. Mitochondrial preparations derive from three independent experiments, and the corresponding 2D gels of the two remaining biological replicates as well as

182 one reference gel each for mitochondrial and chloroplast fractions from *Arabidopsis* cell culture
183 (Mito ref) or leaves (Cp rev) are shown in Supplemental Fig. S1. These three preparations were
184 used for lipidomics with LC-MS/MS (Fig. 3, 5, 6, and S3) and proteomics **(B)**.

185 **B:** Mitochondrial fractions from *Arabidopsis* leaves and cell cultures were analyzed by label-free
186 quantitative shotgun proteomics. Peptide intensities assigned to subcellular compartments
187 were summed-up and averaged results for L-mitos and C-mitos from the three independent
188 experiments were visualized by pie charts (for detailed results see Supplemental Fig. S2 and
189 Supplemental Tab. S1). Blue: mitochondria; green: plastids; gray: others; numbers in %.

190

191 **PC, PE and CL are strongly enriched glycerolipids in plant leaf mitochondria**

192 Glycerolipids are the most abundant lipids not only in mitochondria but also generally in plant
193 tissues, accounting for more than 90 % of the overall lipids in leaves (Li-Beisson et al., 2013;
194 Michaud et al., 2017). Glycerophospholipids are fundamental to all biological membranes, while
195 glyceroglycolipids are critical for photosynthetic membranes and localize mainly in plastids of
196 vegetative tissues (Hölzl and Dörmann, 2019). Therefore, lipids were extracted from leaves and
197 purified mitochondria therefrom to determine the proportion of the major glycerolipid classes
198 in a quantitative approach based on thin layer chromatography followed by gas chromatography
199 coupled to flame ionization detection (TLC-GC/FID, Fig. 2). In L-TE, glyceroglycolipids including
200 monogalactosyldiacylglycerols (MGDG; 38.9 ± 1.1 %) and DGDG (22.3 ± 3.8 %) contribute to the
201 majority of the overall lipids; while glycerophospholipids, PC (35.7 ± 6.0 %) and PE (37.2 ± 0.3 %),
202 are the most abundant lipids in L-mito. CL accounts for 4.0 ± 0.9 % in the lipidome of L-mito;
203 however, it was not detectable in L-TE because of its low abundance in total cellular lipids. PG,
204 as the precursor of CL, consists 5.6 ± 2.1 % of the overall lipids in L-mito.

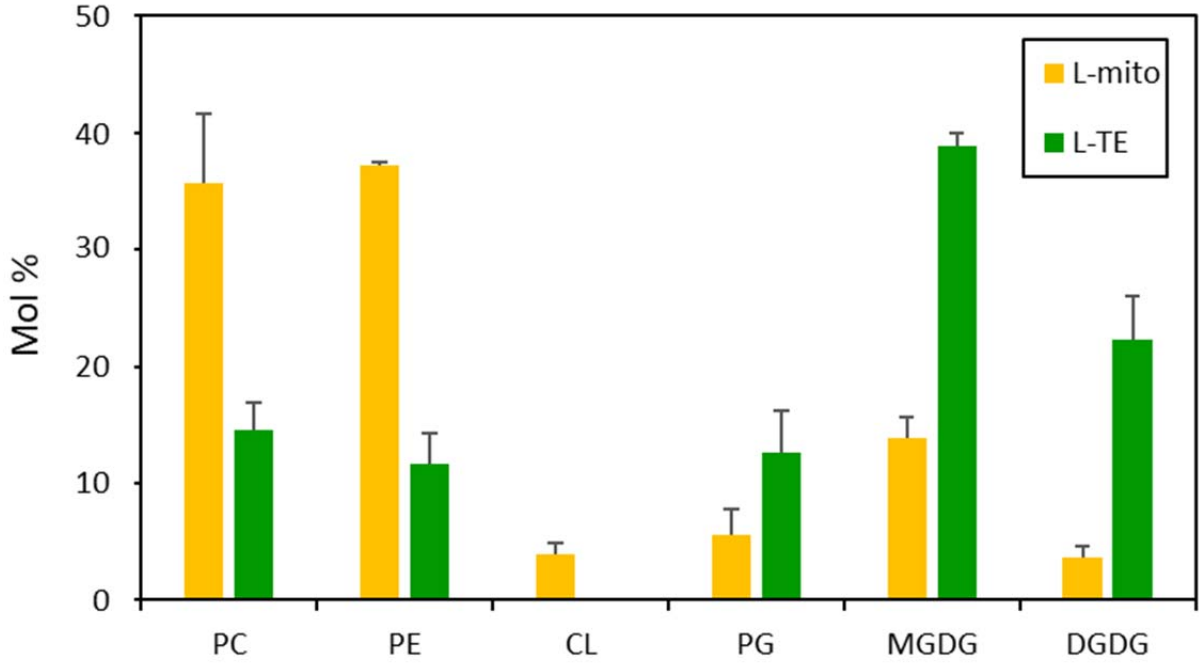


205

206 **Figure 2.** Lipid class profiles of purified mitochondria and total leaf extracts. Glycerolipids of leaf
207 total extract (L-TE) and mitochondria isolated from leaves (L-mito) were analyzed quantitatively
208 by a TLC-GC/FID approach. Data of L-TE represent mean values in mol % from three
209 independent experiments ± SD; data of L-mito represent mean values in mol % from two of the
210 three independent experiments ± SEM. PC, phosphatidylcholine; PE, phosphatidylethanolamine;
211 CL, cardiolipin; PG, phosphatidylglycerol; MGDG, monogalactosyldiacylglycerol; DGDG,
212 digalactosyldiacylglycerol.

213

214 **Specific molecular glycerolipid species are enriched in plant leaf mitochondria**

215 Glycerophospholipids are the most abundant lipids in mitochondria (Fig. 2) (Horvath and Daum,
216 2013; Michaud et al., 2017). Therefore, the molecular species of glycerophospholipids, as well as
217 those of glyceroglycolipids and diacylglycerols, were analyzed from the same samples
218 originating from three independent experiments as for proteomics (Fig. 1) by LC-MS/MS (Fig. 3a).
219 Data are expressed in mol %. The most abundant PC and PE molecular species in mitochondria
220 with the acyl chains 18:2/18:3, 18:2/18:2 and 18:3/18:3 account for more than 60 % in both lipid
221 classes (Fig. 3a; Supplemental Tab. S2). The species 16:0/18:2, 16:0/18:3 of both lipid classes

222 however were depleted by about 50 % in this organelle in comparison to L-TE. PS (18:0/18:2)
223 composes up to 38.3 % in L-mito with an increase of $2^{4.3}$ fold comparing to L-TE. The
224 accumulation of this lipid species was the most remarkable one that was even visible when the
225 fatty acid profiles of the different lipid classes were calculated from the molecular species data,
226 showing an enrichment of 18:0 in mitochondria on the expense of 16:0 (Supplemental Fig. S3).
227 Together the main molecular species of these three lipid classes have a C18/C18 acyl chain
228 composition in common.

**a**

| PC Mol % | L-TE | L-mito | Mean | Log2(FC) |
|---|---|---|---|---|
| * 16:0/16:0 | 0.0 | 0.0 | 0.0 | |
| 16:0/16:1 | 0.2 | 0.1 | 0.2 | |
| ** 16:0/18:1 | 2.1 | 1.0 | 1.5 | -1.1 |
| ** 16:0/18:2 | 20.3 | 11.1 | 15.7 | -0.9 |
| ** 16:0/18:3 | 17.7 | 12.9 | 15.3 | -0.5 |
| * 16:1/16:1 | 0.0 | 0.0 | 0.0 | |
| 16:1/18:0 | 0.0 | 0.0 | 0.0 | |
| 16:1/18:1 | 0.1 | 0.1 | 0.1 | |
| 16:1/18:2 | 0.5 | 0.5 | 0.5 | 0.0 |
| 16:1/18:3 | 0.6 | 0.6 | 0.6 | 0.0 |
| 18:0/18:0 | 0.0 | 0.0 | 0.0 | |
| * 18:0/18:1 | 0.2 | 0.1 | 0.2 | |
| ** 18:0/18:2 | 1.8 | 1.0 | 1.4 | -0.8 |
| ** 18:0/18:3 | 1.4 | 0.7 | 1.1 | -0.9 |
| 18:1/18:1 | 0.4 | 0.4 | 0.4 | |
| 18:1/18:2 | 3.0 | 3.8 | 3.4 | 0.3 |
| 18:1/22:1 | 0.0 | 0.0 | 0.0 | |
| * 18:1/18:3 | 2.7 | 3.7 | 3.2 | 0.4 |
| ** 18:2/18:2 | 13.6 | 18.7 | 16.1 | 0.5 |
| ** 18:2/18:3 | 20.6 | 29.4 | 25.0 | 0.5 |
| 18:2/20:1 | 0.1 | 0.1 | 0.1 | |
| 18:2/20:2 | 0.1 | 0.2 | 0.2 | |
| 18:2/22:0 | 0.0 | 0.0 | 0.0 | |
| 18:3/18:3 | 14.2 | 15.2 | 14.7 | 0.1 |
| 18:3/20:0 | 0.0 | 0.0 | 0.0 | |
| 18:3/20:1 | 0.1 | 0.1 | 0.1 | |
| * 18:3/20:2 | 0.1 | 0.1 | 0.1 | |
| * 18:3/22:0 | | 0.0 | 0.0 | |

| PE Mol % | L-TE | L-mito | Mean | Log2(FC) |
|---|---|---|---|---|
| 16:0/16:0 | 0.0 | 0.0 | 0.0 | |
| 16:0/16:1 | 0.1 | 0.3 | 0.2 | |
| ** 16:0/18:1 | 1.4 | 0.3 | 0.9 | -2.3 |
| ** 16:0/18:2 | 31.1 | 8.0 | 19.6 | -2.0 |
| ** 16:0/18:3 | 19.3 | 5.7 | 12.5 | -1.8 |
| 16:1/18:0 | 0.0 | 0.0 | 0.0 | |
| * 16:1/18:1 | 0.0 | 0.2 | 0.1 | |
| ** 16:1/18:2 | 0.4 | 0.2 | 0.3 | |
| * 16:1/18:3 | 0.3 | 0.2 | 0.2 | |
| 18:0/18:1 | 0.1 | 0.0 | 0.0 | |
| ** 18:0/18:2 | 1.8 | 0.4 | 1.1 | -2.3 |
| ** 18:0/18:3 | 1.1 | 0.4 | 0.8 | -1.3 |
| 18:1/18:1 | 0.1 | 0.2 | 0.2 | |
| * 18:1/18:2 | 3.1 | 2.4 | 2.7 | -0.4 |
| 18:1/18:3 | 1.7 | 1.5 | 1.6 | -0.2 |
| ** 18:2/18:2 | 12.7 | 25.2 | 18.9 | 1.0 |
| ** 18:2/18:3 | 17.5 | 40.3 | 28.9 | 1.2 |
| * 18:2/20:0 | 0.2 | 0.1 | 0.2 | |
| 18:2/20:1 | 0.2 | 0.1 | 0.1 | |
| * 18:2/20:2 | 0.2 | 0.3 | 0.3 | |
| 18:2/22:0 | 0.3 | 0.0 | 0.2 | |
| 18:2/24:0 | 0.2 | 0.0 | 0.1 | |
| 18:2/24:1 | 0.2 | 0.1 | 0.1 | |
| ** 18:3/18:3 | 7.0 | 13.6 | 10.3 | 0.9 |
| 18:3/20:0 | 0.2 | 0.0 | 0.1 | |
| * 18:3/20:1 | 0.1 | 0.1 | 0.1 | |
| 18:3/20:2 | 0.1 | 0.1 | 0.1 | |
| 18:3/22:0 | 0.2 | 0.1 | 0.1 | |
| 18:3/24:0 | 0.1 | 0.1 | 0.1 | |
| 18:3/24:1 | 0.1 | 0.1 | 0.1 | |

| PS Mol % | L-TE | L-mito | Mean | Log2(FC) |
|---|---|---|---|---|
| 16:0/16:0 | 0.9 | 1.1 | 1.0 | 0.2 |
| 16:0/16:1 | 0.6 | 0.3 | 0.4 | |
| ** 16:0/18:0 | 0.4 | 4.6 | 2.5 | 3.4 |
| 16:0/18:1 | 0.6 | 0.6 | 0.6 | 0.1 |
| 16:0/18:2 | 15.5 | 7.7 | 11.6 | -1.0 |
| ** 16:0/18:3 | 26.4 | 5.7 | 16.0 | -2.2 |
| 16:1/16:1 | | 0.0 | 0.0 | |
| 16:1/18:0 | 0.2 | 0.2 | 0.2 | |
| * 16:1/18:1 | | 0.2 | 0.2 | |
| 16:1/18:2 | 0.8 | 0.1 | 0.4 | |
| 16:1/18:3 | 1.0 | 0.2 | 0.6 | -2.1 |
| * 18:0/18:0 | | 0.2 | 0.2 | |
| * 18:0/18:1 | 0.4 | 1.6 | 1.0 | 2.0 |
| ** 18:0/18:2 | 1.9 | 38.3 | 20.1 | 4.3 |
| ** 18:0/18:3 | 2.6 | 12.4 | 7.5 | 2.2 |
| 18:1/18:1 | | 0.1 | 0.1 | |
| 18:1/18:2 | 1.1 | 0.9 | 1.0 | -0.3 |
| 18:1/18:3 | 1.2 | 0.4 | 0.8 | -1.4 |
| 18:2/18:2 | 0.7 | 0.7 | 0.7 | 0.0 |
| * 18:2/18:3 | 3.3 | 0.8 | 2.0 | -2.0 |
| 18:2/24:0 | 6.9 | 4.8 | 5.9 | -0.5 |
| 18:2/24:1 | 11.2 | 9.6 | 10.4 | -0.2 |
| * 18:2/26:0 | 3.3 | 0.4 | 1.9 | -3.0 |
| * 18:2/26:1 | | 2.0 | 2.0 | |
| ** 18:3/18:3 | 5.4 | 0.4 | 2.9 | -3.8 |
| * 18:3/24:0 | 9.8 | 3.6 | 6.7 | -1.5 |
| ** 18:3/24:1 | 5.1 | 1.2 | 3.1 | -2.1 |
| 18:3/26:0 | 0.2 | 0.1 | 0.1 | |
| 18:3/26:1 | 0.7 | 1.6 | 1.2 | 1.2 |

| PI Mol % | L-TE | L-mito | Mean | Log2(FC) |
|---|---|---|---|---|
| 16:0/16:0 | 0.1 | 0.3 | 0.2 | |
| 16:0/16:1 | | 0.5 | 0.5 | |
| 16:0/18:1 | 1.3 | 2.1 | 1.7 | 0.7 |
| ** 16:0/18:2 | 32.0 | 46.2 | 39.1 | 0.5 |
| ** 16:0/18:3 | 48.2 | 37.3 | 42.7 | -0.4 |
| 16:1/16:1 | 0.5 | 0.0 | 0.3 | |
| 16:1/18:1 | | 0.0 | 0.0 | |
| 16:1/18:2 | 0.8 | 0.3 | 0.6 | -1.2 |
| * 16:1/18:3 | 0.9 | 0.3 | 0.6 | -1.5 |
| 18:0/18:0 | | 0.1 | 0.1 | |
| ** 18:0/18:1 | | 0.5 | 0.5 | |
| * 18:0/18:2 | 1.0 | 2.3 | 1.6 | 1.2 |
| 18:0/18:3 | 2.2 | 2.1 | 2.1 | 0.0 |
| ** 18:1/18:1 | | 0.2 | 0.2 | |
| 18:1/18:2 | 0.3 | 0.3 | 0.3 | |
| 18:1/18:3 | 1.0 | 0.8 | 0.9 | -0.4 |
| 18:2/18:2 | 1.7 | 1.9 | 1.8 | 0.2 |
| 18:2/18:3 | 5.6 | 3.7 | 4.6 | -0.6 |
| * 18:3/18:3 | 4.6 | 1.2 | 2.9 | -2.0 |

| $PIP_2$ Mol % | L-TE | L-mito | Mean | Log2(FC) |
|---|---|---|---|---|
| 16:0/18:1 | 7.3 | 8.0 | 7.6 | 0.1 |
| 16:0/18:2 | 58.1 | 48.3 | 53.2 | -0.3 |
| 16:0/18:3 | 27.2 | 34.6 | 30.9 | 0.3 |
| ** 18:1/18:2 | | 4.7 | 4.7 | |
| 18:2/18:2 | 4.3 | 4.4 | 4.3 | 0.0 |
| 18:2/18:3 | 3.1 | | 3.1 | |

| PA Mol % | L-TE | L-mito | Mean | Log2(FC) |
|---|---|---|---|---|
| ** 16:0/16:0 | 0.0 | 1.3 | 0.6 | 5.3 |
| ** 16:0/16:1 | 0.2 | 0.4 | 0.3 | |
| * 16:0/18:0 | 0.0 | 0.2 | 0.1 | |
| 16:0/18:1 | 1.0 | 3.1 | 2.1 | 1.6 |
| ** 16:0/18:2 | 16.2 | 22.2 | 19.2 | 0.5 |
| * 16:0/18:3 | 18.1 | 20.7 | 19.4 | 0.2 |
| ** 16:1/16:1 | 0.0 | 0.1 | 0.0 | |
| 16:1/18:0 | 0.0 | 0.2 | 0.1 | |
| ** 16:1/18:1 | 0.0 | 0.2 | 0.1 | |
| ** 16:1/18:2 | 0.5 | 0.4 | 0.5 | -0.5 |
| * 16:1/18:3 | 0.5 | 0.3 | 0.4 | |
| ** 18:0/18:0 | | 0.1 | 0.1 | |
| ** 18:0/18:1 | 0.1 | 0.2 | 0.1 | |
| ** 18:0/18:2 | 1.0 | 2.2 | 1.6 | 1.1 |
| * 18:0/18:3 | 1.3 | 2.3 | 1.8 | 0.8 |
| ** 18:1/18:1 | 0.1 | 0.7 | 0.4 | |
| * 18:1/18:2 | 2.3 | 3.0 | 2.7 | 0.4 |
| 18:1/18:3 | 2.4 | 2.4 | 2.4 | 0.0 |
| ** 18:2/18:2 | 14.9 | 12.2 | 13.5 | -0.3 |
| ** 18:2/18:3 | 27.3 | 19.8 | 23.5 | -0.5 |
| ** 18:3/18:3 | 14.0 | 8.1 | 11.1 | -0.8 |

| PG Mol % | L-TE | L-mito | Mean | Log2(FC) |
|---|---|---|---|---|
| * 16:0/16:0 | 1.9 | 3.3 | 2.6 | 0.8 |
| 16:0/16:1 | 1.3 | 1.2 | 1.3 | -0.1 |
| ** 16:0/18:0 | 0.2 | 0.7 | 0.4 | |
| 16:0/18:1 | 5.1 | 5.8 | 5.4 | 0.2 |
| ** 16:0/18:2 | 18.1 | 39.3 | 28.7 | 1.1 |
| 16:0/18:3 | 36.0 | 34.6 | 35.3 | -0.1 |
| 16:1/16:1 | | 0.2 | 0.2 | |
| 16:1/18:0 | 0.2 | 0.3 | 0.2 | |
| 16:1/18:1 | 1.0 | 0.9 | 0.9 | -0.1 |
| ** 16:1/18:2 | 3.9 | 1.1 | 2.5 | -1.8 |
| ** 16:1/18:3 | 29.6 | 5.9 | 17.7 | -2.3 |
| 16:3/18:0 | 0.0 | 0.0 | 0.0 | |
| 16:3/18:1 | 0.0 | 0.0 | 0.0 | |
| ** 16:3/18:2 | 0.6 | 0.0 | 0.3 | |
| * 16:3/18:3 | 0.3 | 0.0 | 0.1 | |
| ** 18:0/18:0 | | 0.0 | 0.0 | |
| * 18:0/18:1 | 0.0 | 0.2 | 0.1 | |
| ** 18:0/18:2 | 0.1 | 0.7 | 0.4 | |
| ** 18:0/18:3 | 0.1 | 0.4 | 0.2 | |
| * 18:1/18:1 | 0.0 | 1.4 | 0.7 | 8.0 |
| ** 18:1/18:2 | 0.1 | 0.3 | 0.2 | |
| ** 18:1/18:3 | 0.1 | 0.3 | 0.2 | |
| 18:2/18:2 | 0.2 | 1.0 | 0.6 | 2.4 |
| ** 18:2/18:3 | 0.5 | 1.6 | 1.1 | 1.6 |
| 18:3/18:3 | 0.8 | 0.9 | 0.8 | 0.3 |

| CL Mol % | L-mito |
|---|---|
| 68:4 | 0.2 |
| 68:5 | 0.2 |
| 68:6 | 0.1 |
| 68:7 | 0.0 |
| 70:5 | 0.1 |
| 70:6 | 0.2 |
| 70:7 | 0.3 |
| 70:8 | 0.3 |
| 70:9 | 0.4 |
| 70:10 | 0.3 |
| 72:6 | 0.3 |
| 72:7 | 1.6 |
| 72:8 | 5.9 |
| 72:9 | 14.0 |
| 72:10 | 27.8 |
| 72:11 | 34.7 |
| 72:12 | 13.7 |

**b**

| MGDG Mol % | L-TE | L-mito | Mean | Log2(FC) |
|---|---|---|---|---|
| * 16:0/16:0 | 0.0 | 0.0 | 0.0 | |
| 16:0/16:1 | 0.0 | 0.0 | 0.0 | |
| * 16:0/16:2 | 0.0 | 0.1 | 0.0 | |
| ** 16:0/16:3 | 0.1 | 0.1 | 0.1 | |
| 16:0/18:0 | 0.0 | 0.1 | 0.1 | |
| ** 16:0/18:1 | 0.6 | 1.4 | 1.0 | 1.1 |
| 16:0/18:2 | 0.5 | 0.9 | 0.7 | 0.7 |
| * 16:0/18:3 | 0.8 | 2.3 | 1.6 | 1.5 |
| 16:1/16:1 | 0.0 | 0.0 | 0.0 | |
| 16:1/16:2 | 0.0 | 0.0 | 0.0 | |
| 16:1/16:3 | 0.1 | 0.1 | 0.1 | |
| 16:1/18:0 | 0.1 | 0.1 | 0.1 | |
| * 16:1/18:1 | 0.8 | 0.5 | 0.7 | -0.8 |
| 16:1/18:2 | 1.1 | 1.0 | 1.0 | -0.1 |
| * 16:1/18:3 | 1.3 | 0.9 | 1.1 | -0.5 |
| 16:2/18:0 | 0.0 | 0.0 | 0.0 | |
| 16:2/18:1 | 0.4 | 0.4 | 0.4 | |
| 16:2/18:2 | 1.4 | 1.2 | 1.3 | -0.2 |
| ** 16:2/18:3 | 3.6 | 2.6 | 3.1 | -0.4 |
| 16:3/18:0 | 0.0 | 0.0 | 0.0 | |
| * 16:3/18:1 | 0.3 | 0.2 | 0.3 | |
| ** 16:3/18:2 | 1.6 | 1.1 | 1.3 | -0.6 |
| ** 16:3/18:3 | 63.8 | 52.1 | 57.9 | -0.3 |
| ** 18:0/18:0 | 0.0 | 0.0 | 0.0 | |
| * 18:0/18:1 | 0.0 | 0.1 | 0.0 | |
| ** 18:0/18:2 | 0.0 | 0.2 | 0.1 | |
| ** 18:0/18:3 | 0.1 | 0.3 | 0.2 | |
| 18:1/18:1 | 0.0 | 0.2 | 0.1 | |
| 18:1/18:2 | 0.1 | 0.2 | 0.1 | |
| * 18:1/18:3 | 0.5 | 0.8 | 0.6 | 0.6 |
| * 18:2/18:2 | 0.5 | 1.2 | 0.9 | 1.4 |
| ** 18:2/18:3 | 2.5 | 4.2 | 3.4 | 0.7 |
| * 18:3/18:3 | 19.6 | 27.7 | 23.7 | 0.5 |

| DGDG Mol % | L-TE | L-mito | Mean | Log2(FC) |
|---|---|---|---|---|
| ** 16:0/16:0 | 0.1 | 0.3 | 0.2 | |
| 16:0/16:1 | 0.0 | 0.0 | 0.0 | |
| 16:0/16:2 | 0.0 | 0.1 | 0.0 | |
| 16:0/16:3 | 0.0 | 0.1 | 0.0 | |
| ** 16:0/18:0 | 0.2 | 0.1 | 0.1 | |
| 16:0/18:1 | 1.3 | 1.2 | 1.2 | -0.1 |
| * 16:0/18:2 | 5.3 | 3.7 | 4.5 | -0.5 |
| 16:0/18:3 | 11.8 | 11.4 | 11.6 | -0.1 |
| 16:1/16:1 | | 0.0 | 0.0 | |
| 16:1/16:2 | | 0.0 | 0.0 | |
| 16:1/16:3 | | 0.0 | 0.0 | |
| 16:1/18:0 | 0.0 | 0.0 | 0.0 | |
| 16:1/18:1 | 0.1 | 0.1 | 0.1 | |
| 16:1/18:2 | 0.2 | 0.2 | 0.2 | |
| 16:1/18:3 | 0.5 | 0.5 | 0.5 | -0.1 |
| 16:2/18:0 | 0.0 | 0.1 | 0.0 | |
| 16:2/18:1 | 0.1 | 0.1 | 0.1 | |
| 16:2/18:2 | 0.2 | 0.3 | 0.3 | |
| 16:2/18:3 | 1.9 | 1.4 | 1.7 | -0.4 |
| 16:3/18:0 | 0.0 | 0.1 | 0.1 | |
| 16:3/18:1 | 0.0 | 0.1 | 0.0 | |
| * 16:3/18:2 | 0.2 | 0.4 | 0.3 | |
| * 16:3/18:3 | 10.1 | 14.0 | 12.0 | 0.5 |
| 18:0/18:0 | | 0.0 | 0.0 | |
| ** 18:0/18:1 | 0.0 | 0.1 | 0.1 | |
| 18:0/18:2 | 0.2 | 0.2 | 0.2 | |
| 18:0/18:3 | 0.8 | 1.0 | 0.9 | 0.4 |
| 18:1/18:1 | 0.0 | 0.0 | 0.0 | |
| 18:1/18:2 | 0.1 | 0.1 | 0.1 | |
| ** 18:1/18:3 | 0.8 | 1.0 | 0.9 | 0.3 |
| 18:2/18:2 | 0.4 | 0.4 | 0.4 | |
| 18:2/18:3 | 3.2 | 3.1 | 3.1 | 0.0 |
| 18:3/18:3 | 62.2 | 60.0 | 61.1 | -0.1 |

**c**

| DAG Mol % | L-TE | L-mito | Mean | Log2(FC) |
|---|---|---|---|---|
| * 16:0/16:0 | 0.2 | 0.8 | 0.5 | 2.2 |
| 16:0/16:1 | 0.3 | 0.2 | 0.3 | |
| 16:0/18:0 | 0.9 | 0.7 | 0.8 | -0.3 |
| 16:0/18:1 | 2.6 | 2.1 | 2.4 | -0.3 |
| ** 16:0/18:2 | 29.8 | 20.4 | 25.1 | -0.5 |
| 16:0/18:3 | 18.6 | 17.7 | 18.1 | -0.1 |
| 16:0/20:0 | 0.1 | 0.1 | 0.1 | |
| 16:0/20:1 | 0.1 | 0.1 | 0.1 | |
| 16:0/22:0 | 0.1 | 0.1 | 0.1 | |
| 16:0/22:1 | 0.0 | 0.1 | 0.0 | |
| 16:0/24:0 | 0.1 | 0.2 | 0.1 | |
| 16:0/24:1 | 0.1 | 0.0 | 0.1 | |
| 16:1/16:1 | 0.0 | 0.1 | 0.1 | |
| 16:1/18:0 | 0.0 | 0.0 | 0.0 | |
| 16:1/18:1 | 0.2 | 0.3 | 0.2 | |
| 16:1/18:2 | 0.6 | 0.7 | 0.6 | 0.1 |
| 16:1/18:3 | 0.5 | 0.6 | 0.6 | 0.4 |
| 16:1/20:0 | 0.1 | 0.1 | 0.1 | |
| 16:1/20:1 | 0.1 | 0.1 | 0.1 | |
| 16:1/22:0 | 0.0 | 0.1 | 0.0 | |
| 16:1/22:1 | 0.1 | 0.1 | 0.1 | |
| 16:1/24:1 | 0.1 | 0.2 | 0.1 | |
| 18:0/18:0 | 0.8 | 0.4 | 0.6 | -1.0 |
| 18:0/18:1 | 0.3 | 0.3 | 0.3 | |
| * 18:0/18:2 | 2.9 | 2.0 | 2.5 | -0.5 |
| 18:0/18:3 | 1.4 | 1.7 | 1.6 | 0.3 |
| 18:0/20:0 | 0.1 | 0.0 | 0.0 | |
| 18:0/20:1 | 0.0 | 0.0 | 0.0 | |
| 18:0/22:0 | 0.1 | 0.0 | 0.0 | |
| 18:0/22:1 | 0.1 | 0.0 | 0.1 | |
| 18:0/24:0 | 0.1 | 0.0 | 0.1 | |
| 18:0/24:1 | 0.0 | 0.0 | 0.0 | |

| DAG Mol % | L-TE | L-mito | Mean | Log2(FC) |
|---|---|---|---|---|
| * 18:1/18:1 | 0.3 | 0.6 | 0.5 | 0.9 |
| * 18:1/18:2 | 2.4 | 3.2 | 2.8 | 0.4 |
| 18:1/18:3 | 2.7 | 2.8 | 2.7 | 0.0 |
| 18:1/20:0 | 0.1 | 0.0 | 0.1 | |
| 18:1/20:1 | 0.0 | 0.0 | 0.0 | |
| 18:1/22:0 | 0.0 | 0.0 | 0.0 | |
| 18:1/22:1 | 0.1 | 0.1 | 0.1 | |
| 18:1/24:0 | 0.0 | 0.0 | 0.0 | |
| 18:1/24:1 | 0.0 | 0.0 | 0.0 | |
| 18:2/18:2 | 10.1 | 9.5 | 9.8 | -0.1 |
| * 18:2/18:3 | 14.9 | 17.7 | 16.3 | 0.3 |
| 18:2/20:0 | 0.1 | 0.2 | 0.1 | |
| 18:2/20:1 | 0.3 | 0.2 | 0.2 | |
| 18:2/22:0 | 0.2 | 0.2 | 0.2 | |
| 18:2/22:1 | 0.3 | 0.2 | 0.2 | |
| ** 18:2/24:0 | 0.2 | 0.4 | 0.3 | |
| * 18:2/24:1 | 0.1 | 0.2 | 0.2 | |
| ** 18:3/18:3 | 6.3 | 13.7 | 10.0 | 1.1 |
| 18:3/20:0 | 0.1 | 0.1 | 0.1 | |
| 18:3/20:1 | 0.2 | 0.2 | 0.2 | |
| 18:3/22:0 | 0.2 | 0.2 | 0.2 | |
| 18:3/22:1 | 0.1 | 0.1 | 0.1 | |
| * 18:3/24:0 | 0.1 | 0.3 | 0.2 | |
| * 18:3/24:1 | 0.1 | 0.2 | 0.1 | |
| 20:0/20:0 | 0.0 | 0.0 | 0.0 | |
| 20:0/20:1 | 0.0 | 0.0 | 0.0 | |
| 20:0/22:0 | 0.1 | 0.0 | 0.1 | |
| 20:0/22:1 | 0.0 | 0.0 | 0.0 | |
| * 20:0/24:0 | 0.0 | 0.0 | 0.0 | |
| * 20:0/24:1 | 0.1 | 0.0 | 0.0 | |
| 20:1/20:1 | 0.0 | 0.0 | 0.0 | |
| 20:1/22:0 | 0.0 | 0.0 | 0.0 | |
| 20:1/24:0 | 0.0 | 0.0 | 0.0 | |
| 20:1/24:1 | 0.0 | 0.0 | 0.0 | |
| 20:0/22:1 | 0.0 | 0.0 | 0.0 | |
| 22:0/22:0 | 0.0 | 0.1 | 0.0 | |
| 22:0/22:1 | 0.0 | 0.0 | 0.0 | |
| * 22:0/24:0 | 0.0 | 0.2 | 0.1 | |
| 22:0/24:1 | 0.0 | 0.0 | 0.0 | |
| 22:1/22:1 | 0.0 | 0.0 | 0.0 | |
| 22:1/24:0 | 0.0 | 0.0 | 0.0 | |
| 22:1/24:1 | 0.1 | 0.1 | 0.1 | |
| 24:0/24:0 | 0.0 | 0.0 | 0.0 | |
| 24:0/24:1 | 0.0 | 0.0 | 0.0 | |
| 24:1/24:1 | | 0.0 | 0.0 | |

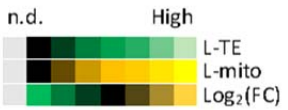


229

230 **Figure 3.** Profiles of the distribution and fold changes of the molecular glycerolipid species
231 between L-mito and L-TE. Heat map visualizations of (a) glycerophospholipids, (b)
232 glyceroglycolipids and (c) diacylglycerols illustrate the difference of species distribution based on
233 LC-MS/MS analyses. Each lipid class is represented by one set of joined columns, only DAG is
234 divided into two sets due to space constraints. Identity of columns in each set from left to right:
235 Column 1 lists the individual lipid class and the identity of the detected molecular lipid species.
236 Column 2 (L-TE) lists the respective distribution of each molecular species in L-TE, expressed as
237 the mean of its relative values in mol % in the three independent experiments also used for
238 proteomics and for sphingolipid and sterol analysis (Figs. 1, 5 and 6, Supplemental Tab. S1).
239 Column 3 (L-mito) lists the respective distribution of each molecular species in L-mito, expressed
240 as the mean of its relative values (mol %) in the three independent experiments also used for
241 proteomics. Column 4 lists the mean distribution of both sample types, and column 5 ($Log_2$(FC))
242 lists the binary logarithm of fold change. Binary logarithm was applied when the mean values
243 are higher than 0.5 to inspect the fold changes (FC) between L-mito and L-TE. The heat map
244 colors represent mean intensity values according to the color map on the low right-hand side.
245 One and two asterisks (*, **) indicate p values < 0.05 and < 0.01, respectively, by Student's t-
246 test. PC, phosphatidylcholine; PE, phosphatidylethanolamine; PS: phosphatidylserine; PI:
247 phosphatidylinositol; PA phosphatidic acid; DAG: Diacylglycerol; CL, cardiolipin; PG,
248 phosphatidylglycerol; MGDG, monogalactosyldiacylglycerol; DGDG, digalactosyldiacylglycerol.

249

250 An important intermediate in glycerolipid metabolism is phosphatidic acid (PA), serving as
251 precursor or product for numerous glycerolipids including PC, PE, PG, phosphatidylinositol (PI)
252 and DAG. PA (16:0/18:2), PA (16:0/18:3) and PA (18:2/18:3) are the most abundant PA species in
253 both fractions, L-mito and L-TE. Notably, only a minor molecular PA species (16:0/16:0; 1.3 mol
254 %) accumulates preferentially in mitochondria with an enrichment of $2^{5.3}$ fold comparing to L-TE.
255 DAG as the other important lipid intermediate displays a higher complexity in its species profile.
256 DAG (16:0/18:2), DAG (16:0/18:3), DAG (18:2/18:3) and DAG (18:3/18:3) build a substantial
257 amount (>65 mol %) of the DAG profile in L-mito (Fig. 3c). As in case of PA, only the minor DAG
258 species (16:0/16:0) shows a $2^{2.2}$ fold increase in L-mito compared to L-TE.

259 PG is formed from PA in the envelopes of plastids and mitochondria and serves as precursor for
260 the mitochondrial lipid CL (Babiychuk et al., 2003). Hydrolysis and condensation of PG lead to
261 the formation of DAG and CL correspondingly. PG (16:0/18:2) and PG (16:0/18:3) are the major
262 species in L-mito, but only the former species is enriched in mitochondria ($2^{1.1}$ fold). In addition,
263 unsaturated PG species are significantly enriched in L-mito, which contribute to the structures of
264 the down-stream CL molecules. CL (72:10) and CL (72:11), composed of 18:2 and 18:3 acyl
265 chains, are the most abundant CL (Fig. 3a).

266 Glycerophospholipids serve not only as membrane building blocks but are also important
267 precursors for signaling molecules in the cell. PI, phosphatidylinositol monophosphate (PIP) and
268 phosphatidylinositol bisphosphate ($PIP_2$) exert regulatory functions in cell development and
269 polarity determination (Heilmann, 2016). In L-mito, molecular species with 16:0/18:2 and
270 16:0/18:3 acyl chains compose up to 80 % of PI and $PIP_2$; yet PIP was not detectable in L-mito.
271 PI (16:0/16:1) and PI (18:0/18:1) were only detectable in the mitochondrial extracts, and
272 PI (18:0/18:2) is significantly enriched in L-mito for $2^{1.2}$ fold in comparison to L-TE (Fig. 3a). On
273 the other hand, we obtained higher signals of $PIP_2$ (18:1/18:2) in L-mito.

274 Glyceroglycolipids carry carbohydrate residues as their head groups; for instance, the galactose-
275 containing lipids, MGDG and DGDG contain one and two galactoses, respectively (Hölzl and
276 Dörmann, 2019). MGDG (16:3/18:3) and DGDG (18:3/18:3) are the major components of the
277 overall glyceroglycolipids in both L-TE and L-mito (Fig. 3b). The amount of MGDG (16:0/18:3)
278 and MGDG (18:2/18:2) are specifically elevated in L-mito for $2^{1.5}$ and $2^{1.4}$ folds, respectively,
279 compared to L-TE. In contrast, the species MGDG (16:1/18:1) and MGDG (16:3/18:2) are
280 significantly decreased in L-mito. In summary, the major mitochondrial lipids PC, PE, PS and CL
281 consist primarily of C18/C18 species, while PI, PIP2 and PG consist primarily of C16/C18 species
282 and the lipid precursors DAG and PA resemble a mixture of both backbones.

283 **Proteomic analyses provides insights into the leaf mitochondrial glycerolipid metabolism**
284 **capacity**

285 To further analyze the proteome of the mitochondrial fractions listed in Supplemental Tab. S1,
286 their protein composition was investigated for enzymes from lipid metabolism. Subsequently,
287 their biological function and the subcellular localization were retrieved from The Arabidopsis

288 Information Resource (TAIR) and the Subcellular localization database for Arabidopsis proteins
289 (SUBAcon) databases (Supplemental Fig. S4).

290 About 40 proteins involved in the biosynthesis and modification of fatty acids and more complex
291 lipids were identified in mitochondrial extracts (Supplemental Tab. S3). Four enzymes from
292 glycerophospholipid metabolism were detected in all mitochondrial fractions (Fig. 4). Two
293 glycerol-3-phosphate dehydrogenases were identified (SDP6 and GPDHp), being involved in an
294 early step of glycerophospholipid biosynthesis. Phosphoethanolamine cytidylyltransferase (PECT)
295 was detected in our study by similar abundances in the L-mito and C-mito samples. CL is
296 synthesized after the condensation of PG and CDP-DAG by CL synthase (CLS) or after the
297 transacylation of monolyso-CL by monolysocardiolipin acyltransferase (LCLAT or Tafazzin)(Xu et
298 al., 2006). CLS and Tafazzin were identified in the shotgun proteomic analysis in this study with a
299 higher abundance in C-mito compared to L-mito. PG is synthesized from PA via CDP-DAG by
300 phosphatidylglycerophosphate synthase 1 (PGP1) (Xu et al., 2002) and it was only detected in C-
301 mito samples. Phosphatidylserine decarboxylase 1 (PSD1) synthesizes PE by decarboxylating the
302 headgroup of PS (Birner et al., 2001; Nerlich et al., 2007). Again in our study PSD1 was only
303 detected in C-mito samples. Interestingly PE and PC can be interconverted into each other via
304 PA and the detected phospholipase Dα1 (PLDα1) enzyme activity. PLDα1 was preferentially
305 found in C-mito samples. PIP and $PIP_2$ can be degraded by *myo*-inositol polyphosphate 1-
306 phosphatase (SAL1). Although many enzymes involved in phosphoinositide metabolism have
307 been annotated to localize in mitochondria, only SAL1 was identified in our approach in the C-
308 mito samples.

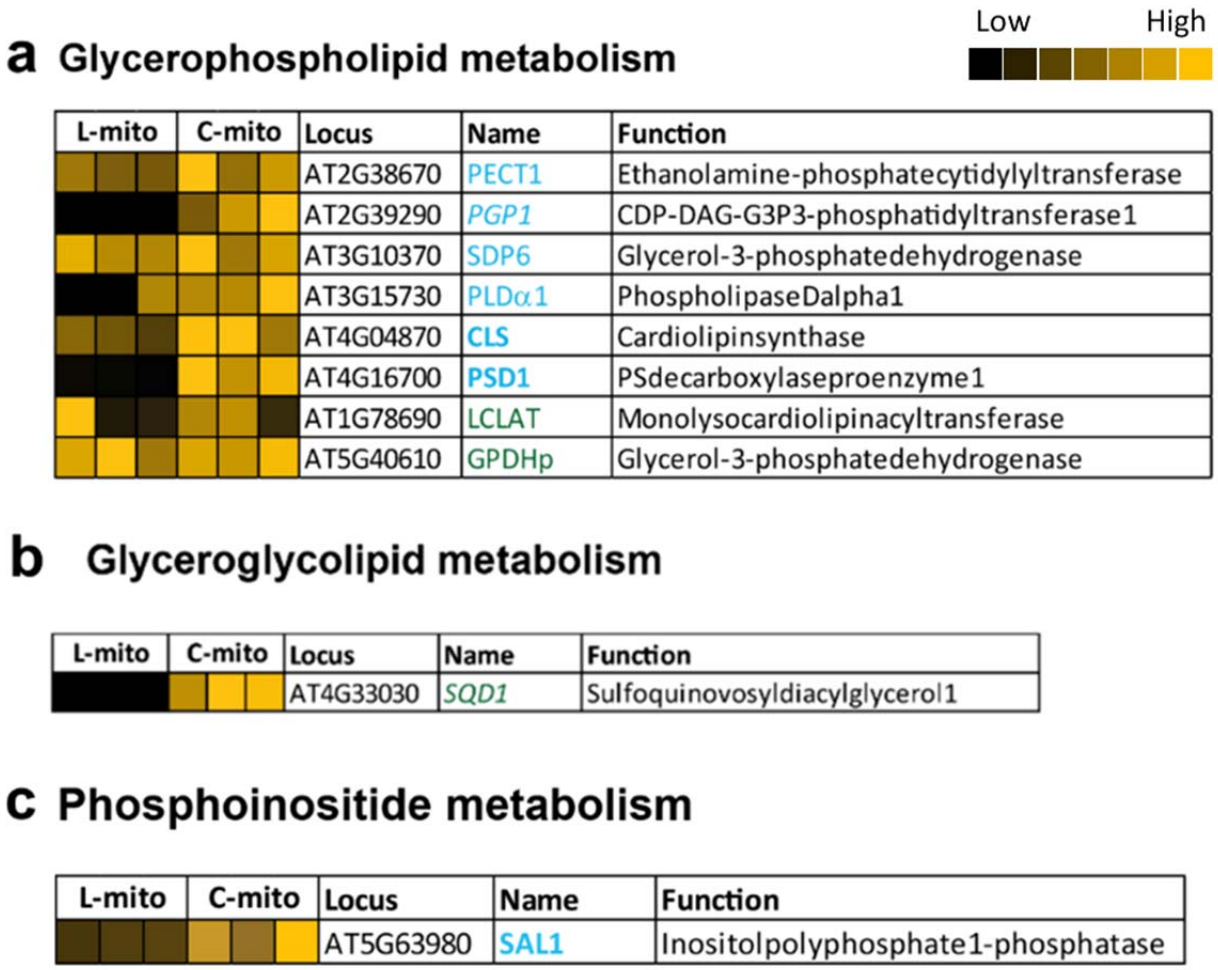


**Figure 4.** Mitochondrial localized proteins that are related to glycerolipid biosynthesis. (a) Glycerophospholipid, (b) glyceroglycolipid and (c) phosphoinositide metabolism. Proteins identified and/or localized in mitochondria were labeled (i) blue: proteins identified in the proteomic analysis of this study and also predicted to localize in mitochondria, (ii) green: proteins identified in the proteomic analysis of this study in mitochondria but predicted to localize in other organelles, (iii) bold font: exclusively localized in mitochondria and (iv) italic font: only identified in one of the mitochondrial populations. Heat maps visualize the protein abundance of three independent experiments of mitochondria purified from leaves and cell cultures from Fig. 1 and listed in Supplemental Tabs. S1 and S3. The heat map colors represent mean intensity values according to the color map on the top right-hand side. Predicted protein localization was based on The Arabidopsis Information Resource (TAIR; www.arabidopsis.org) and the Subcellular localization database for Arabidopsis proteins (SUBAcon; www.suba.live).

322

323 The biosynthesis of glyceroglycolipids takes place in the plastids envelopes by MGDG and DGDG
324 synthases (MGDs and DGDs), respectively (Hölzl and Dörmann, 2019). MGDG is generated by
325 adding a galactose head group to DAG; subsequent addition of another galactose by DGD1
326 generates DGDG. The detected specific species profiles of mitochondrial glyceroglycolipids may
327 suggest at least for a specific transport from plastids to mitochondria (Fig. 3b). The sulfolipid
328 SQDG is synthesized in two steps. Uridine diphosphate (UDP)-glucose is first combined with a
329 sulfite by UDP-sulfoquinovose synthase 1 (SQD1), followed by transferring the sulfoquinovose
330 head group to DAG and thus forms SQDG. Although SQD1 was identified in the C-mito samples
331 in this study, we did not detect SQDG lipids in any of the mitochondrial samples. Together we
332 could exclusively localize three biosynthetic steps to mitochondria: (i) CLS and catalyzing the
333 formation of CL as well as (ii) PSD1 and (iii) PECT1 facilitating PE formation.

334 **Specific molecular sphingolipid and sterol species suggest a function in mitochondria**

335 Sphingolipids and sterols are important modulators of membrane microdomains and play
336 critical roles in regulating the balance between cell survival and apoptosis. Therefore, we
337 profiled next their mitochondrial compositions in comparison to the total lipidome of leaves in
338 the same samples that were used for proteomics and glycerolipid analysis (Figs. 1 and 3) by LC-
339 MS/MS (Figs. 5 and 6) and expressed the lipid profiles in mol %. For sphingolipids both simple
340 and complex sphingolipids were measured, including long-chain bases (LCB), phosphorylated
341 LCB (LCB-P), ceramides (Cer), glucosylceramides (GlcCer) and glycosyl inositol
342 phosphoceramides (GIPC) (Fig. 5). All sphingolipids have LCBs, 18-carbon amino-alcohols, as
343 their backbones. Phytosphingosine (18:0;3), hosting three hydroxyl groups, is the most
344 abundant free LCB in both L-mito and L-TE (Fig. 5a). However, dihydrosphingosine (18:0;2) is
345 highly enriched in L-mito as well as phosphorylated dihydrosphingosine (18:0;2-P), which is the
346 major component in the LCB-P pool of L-mito (64.7 %). LCBs can be further *N*-acylated to
347 generate Cer, the basic structure of complex sphingolipid classes. Addition of glucoses to Cer
348 generates GlcCer, following sequential extension of phosphoinositol, hexose and/or hexose
349 derivatives generate series of GIPCs. Series 0, A and B GIPCs carry one, two and three additional
350 hexoses on the head groups of inositol phosphoceramides, respectively (Cacas et al., 2012;

351 Haslam and Feussner, 2022). Similar to LCB and LCB-P, only specific species were enriched in L-
352 mito (Fig. 5b): Cer (18:0;3/24:0;1), GlcCer (18:1;2/24:1;1) and series A hexose-carrying GIPC (H-
353 GIPC) (18:1;3/24:1;1). Remarkably, GIPCs were only detectable in mitochondrial samples (both
354 L-mito and C-mito) in our approach. However, proteins related to sphingolipid metabolism were
355 neither identified in plant mitochondria via proteomic analyses, nor retrieved from online
356 databases.

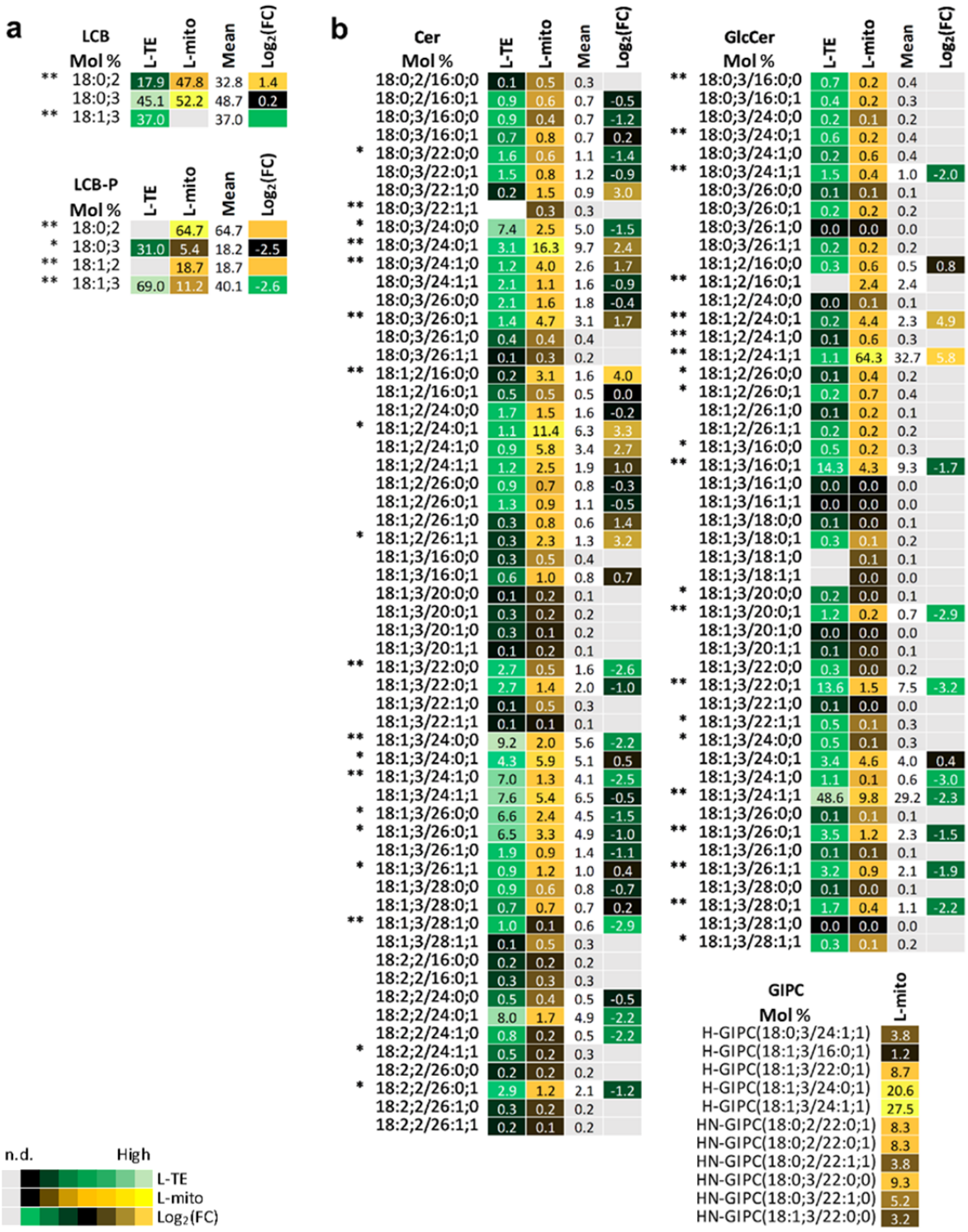


**Figure 5.** Profiles of the distribution and fold changes of the molecular sphingolipid species between L-mito and L-TE. Heat map visualizations of (a) long chain bases, long chain base-phosphates and (b) complex sphingolipids illustrate the difference of species distribution based on LC-MS/MS analyses. Each lipid class is represented by one set of joined columns. Identity of

362 columns in each set from left to right: Column 1 lists the individual lipid class and the identity of
363 the detected molecular lipid species. Column 2 (L-TE) lists the respective distribution of each
364 molecular species in L-TE, expressed as the mean of its relative values (mol %) in the three
365 independent experiments also used for proteomics and for glycerolipid and sterol analysis
366 (Figs. 1, 3 and 6, Supplemental Tab. S1). Column 3 (L-mito) lists the respective distribution of
367 each molecular species in L-mito, expressed as the mean of its relative values (mol %) in the
368 three independent experiments also used for proteomics. Column 4 lists the mean distribution
369 of both sample types, and column 5 ($Log_2$(FC)) lists the binary logarithm of fold change. Binary
370 logarithm was applied when the mean values are higher than 0.5 to inspect the fold changes (FC)
371 between L-mito and L-TE. The heat map colors represent mean intensity values according to the
372 color map on the low left-hand side. One and two asterisks (*, **) indicate p values < 0.05 and <
373 0.01, respectively, by Student's t-test. LCB, long-chain base; LCB-P, long chain base-phosphate;
374 Cer, ceramide; GlcCer, glycosylceramide; GIPC, glycosyl inositol phosphoceramide.

375

376 The common structure of sterols is a four-ring system, cyclopentanoperhydrophenanthrene,
377 with possible conjugation of hydroxyl groups and acyl chains. In plants, a complex mixture of
378 sterols can be found, including brassicasterol, campesterol, cholesterol, sitosterol and
379 stigmasterol (Cacas et al., 2012). Campesterol was identified as major free sterol with 61.7 % in
380 L-mito (Fig. 6). From the group of steryl glycosides cholesteryl and isofucosteryl glycoside
381 accumulated preferentially in L-mito. Considering SE, 16:0 and 18:0 containing cholesteryl esters
382 were enriched $2^{3.4}$ and $2^{5.3}$ folds, respectively, in L-mito. For ASG however the situation was
383 blurred. DWF1 was the only protein related to sterol metabolism that we identified in plant
384 mitochondria via proteomic analyses. In summary, we observed an accumulation of GIPCs and
385 free campersterol in leaf mitochondria.

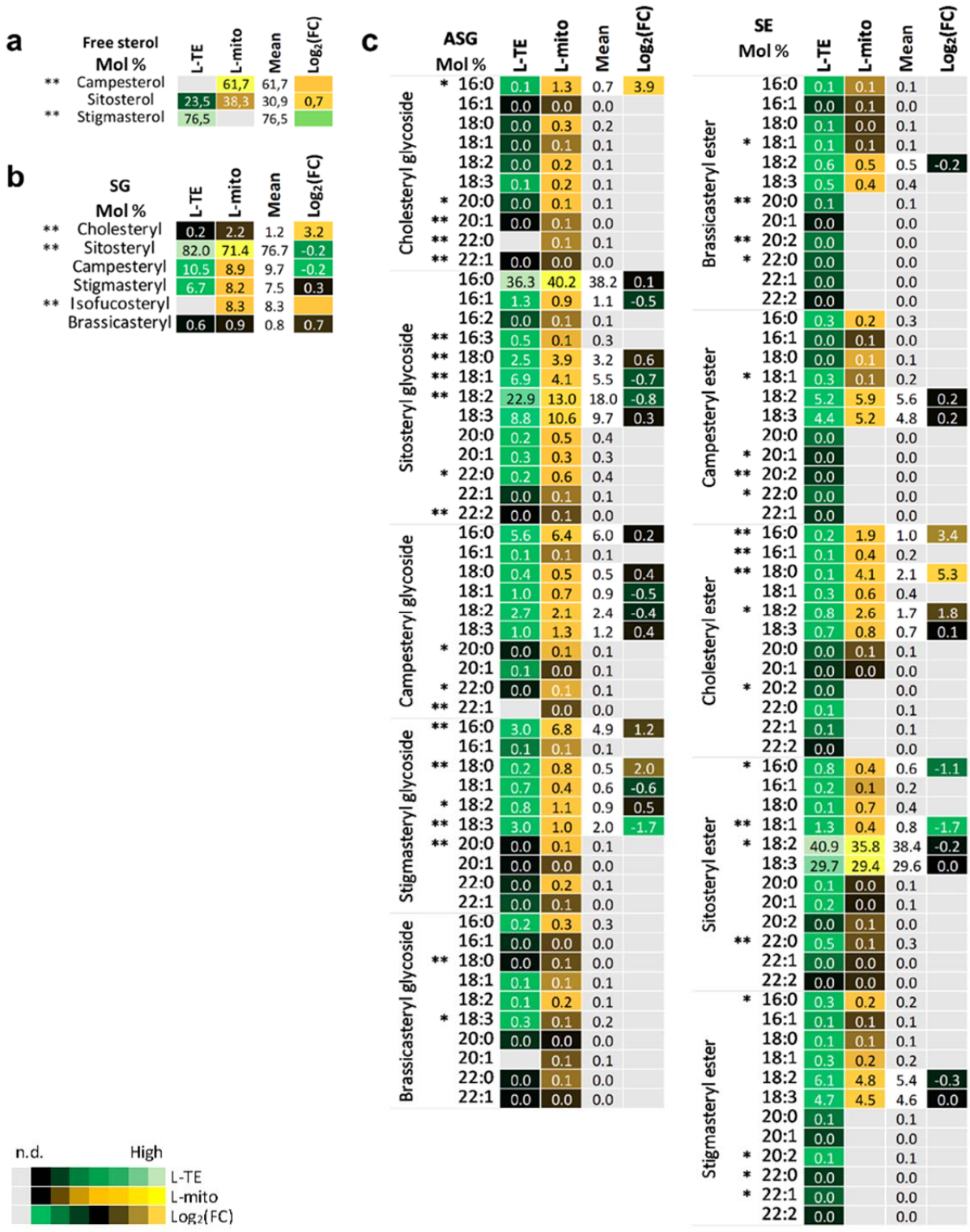


**Figure 6.** Profiles of the distribution and fold changes of the molecular sterol species between L-mito and L-TE. Heat map visualizations of (a) free sterols (b) steryl glycosides (SG) and (c) acylated steryl glycosides (ASG) and steryl esters (SE) illustrate the difference of species distribution based on LC-MS/MS analyses. Each lipid class is represented by one set of joined

391 columns. Identity of columns in each set from left to right: Column 1 lists the individual lipid
392 class and the identity of the detected molecular lipid species. Column 2 (L-TE) lists the respective
393 distribution of each molecular species in L-TE, expressed as the mean of its relative values (mol
394 %) in the three independent experiments also used for proteomics and for glycerolipid and
395 sphingolipid analysis (Figs. 1, 3 and 5, Supplemental Tab. S1). Column 3 (L-mito) lists the
396 respective distribution of each molecular species in L-mito, expressed as the mean of its relative
397 values (mol %) in the three independent experiments also used for proteomics. Column 4 lists
398 the mean distribution of both sample types, and column 5 ($Log_2$(FC)) lists the binary logarithm of
399 fold change. The heat map colors represent mean intensity values according to the color map on
400 the low left-hand side. Binary logarithm was applied when the mean values are higher than 0.5
401 to inspect the fold changes (FC) between L-mito and L-TE. One and two asterisks (*, **) indicate
402 p values < 0.05 and < 0.01, respectively, by Student's t-test.

403 Mitochondria harbor various additional metabolic pathways for the synthesis of lipophilic
404 molecules. More than 20 fatty acid biosynthesis-related proteins were identified in our
405 mitochondrial proteome (Supplemental Fig. S5). They contribute to the synthesis of lipoic acid,
406 ubiquinone and other terpenoid-quinones. Abundance, function and predicted localization of
407 these proteins are specified in Supplemental Tab. S1 and S3.

408 **Lipid molecules can be imported by mitochondria**

409 Transport of DGDG from plastids to mitochondria and reallocation of PE from IM to OM via the
410 MTL complex have been demonstrated under phosphate-depleting conditions (Michaud et al.,
411 2016). The MTL complex has more than 200 subunits and 11 have been verified to associate
412 physically with the core subunits, Mic60 and Tom40, as previously shown by immunoblotting
413 (Michaud et al., 2016; Li et al., 2019). In our mitochondrial proteome listed in Supplemental Tab.
414 S1, 186 of the subunits (87 %) were identified including all the 11 verified ones (Fig. 7,
415 Supplemental Tab. S4). The newly identified MTL subunit, DGS1, which links mitochondrial
416 protein to lipid transport, is present in all mitochondrial extracts.

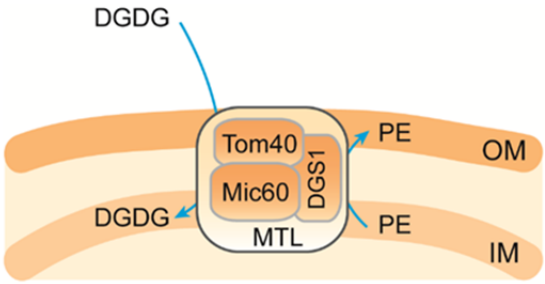


| L-mito | C-mito | Locus | Name | Description |
|---|---|---|---|---|
| | | AT1G06530 | PMD2 | Peroxisomal and mitochondrial division factor 2 |
| | | AT1G27390 | TOM20-2 | Translocase of outer membrane 20 kDa subunit 2 |
| | | AT2G37410 | TIM17-2 | Translocase inner membrane subunit 17-2 |
| | | AT2G42210 | B14.7 | Mitochondrial import inner membrane translocase subunit family protein |
| | | AT3G20000 | TOM40 | Translocase of the outer mitochondrial membrane 40 kDa |
| | | AT3G27080 | TOM20-3 | Translocase of outer membrane 20 kDa subunit 3 |
| | | AT4G39690 | Mic60 | Mitochondrial contact site and cristae organizing system subunit |
| | | AT5G12290 | DGS1 | dgd1 suppressor 1 |
| | | AT5G13430 | RISP | Ubiquinol-cytochrome c reductase iron-sulfur subunit |
| | | AT5G40930 | TOM20-4 | Translocase of outer membrane 20 kDa subunit 4 |
| | | ATMG00160 | COX2 | Cytochrome oxidase 2 |

| L-mito | C-mito | Locus | Name | Function |
|---|---|---|---|---|
| | | AT3G19820 | DWF1 | Delta(24)-sterolreductase |

Low High

**Figure 7.** MTL complex-associated proteins in mitochondria. Our proteomic analyses covered 186 of the 214 hypothetical subunits in the MTL complex (listed in Supplemental Tab. S4); 11 have been investigated by immunoblotting approaches in previous studies. Heat maps visualize the protein abundance of three independent experiments of mitochondria purified from leaves and cell cultures. The heat map colors represent mean intensity values according to the color map on the low right-hand side.

In addition, at least 10 outer envelope (OE)-localized proteins from plastids were co-purified with mitochondria, with higher abundance in C-mito (Fig. 8, Supplemental Tab. S5). They account for 2.1 % (10/471) of the identified plastidial proteins, which are enriched in comparison to the proportion of OE-localized proteins in plastids (46/3002, 1.5 %) (Inoue, 2007, 2011; Simm et al., 2013; Kim et al., 2019). The enrichment of OE-localized proteins in mitochondrial extracts suggest a close physical interaction between mitochondria and plastidial OE membrane. For instance, the membrane contact sites, which were not disrupted during the

432 isolation procedure, and therefore are present in the mitochondrial samples as membrane
433 patches.

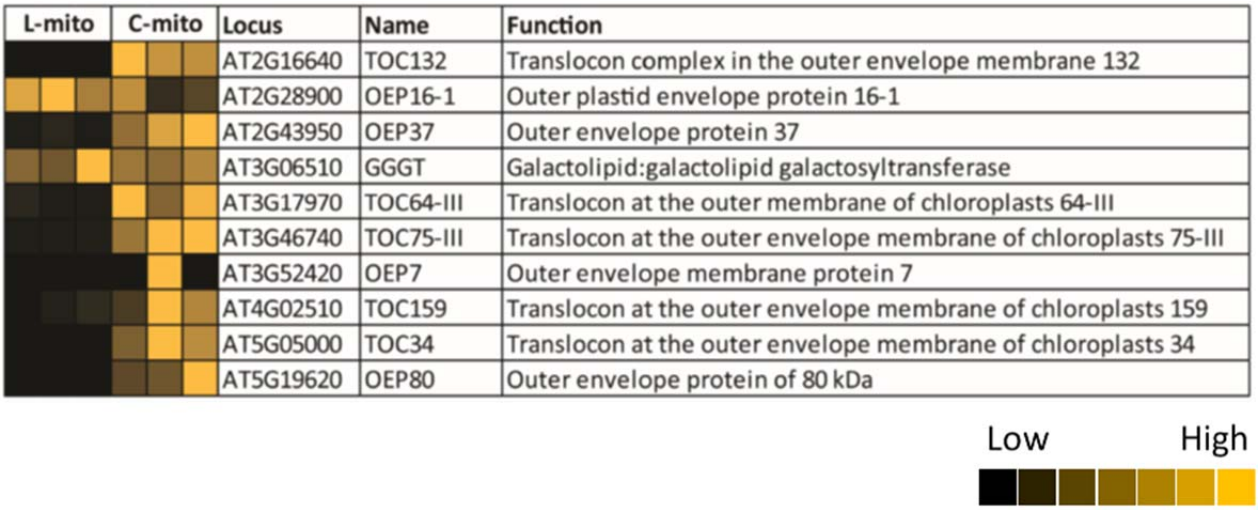

| L-mito | C-mito | Locus | Name | Function |
|---|---|---|---|---|
| | | AT2G16640 | TOC132 | Translocon complex in the outer envelope membrane 132 |
| | | AT2G28900 | OEP16-1 | Outer plastid envelope protein 16-1 |
| | | AT2G43950 | OEP37 | Outer envelope protein 37 |
| | | AT3G06510 | GGGT | Galactolipid:galactolipid galactosyltransferase |
| | | AT3G17970 | TOC64-III | Translocon at the outer membrane of chloroplasts 64-III |
| | | AT3G46740 | TOC75-III | Translocon at the outer envelope membrane of chloroplasts 75-III |
| | | AT3G52420 | OEP7 | Outer envelope membrane protein 7 |
| | | AT4G02510 | TOC159 | Translocon at the outer envelope membrane of chloroplasts 159 |
| | | AT5G05000 | TOC34 | Translocon at the outer envelope membrane of chloroplasts 34 |
| | | AT5G19620 | OEP80 | Outer envelope protein of 80 kDa |



434

435 **Figure 8.** Identified plastid outer envelope proteins in mitochondrial extracts. Our proteomic
436 analyses identified 10 outer envelope-localized proteins (listed in Supplemental Tab. S5). Heat
437 maps visualize the protein abundance of three independent experiments of mitochondria
438 purified from leaves and cell cultures. The heat map colors represent mean intensity values
439 according to the color map on the left-hand side.

440

441

442 **Discussion**

443 In this study, we present an in-depth dataset of lipid molecular species from glycerolipids,
444 sphingolipids and sterols of Arabidopsis leaf mitochondria. With the assistance of online
445 resources, we assigned and confirmed central lipid biosynthesis steps within these
446 mitochondrial fractions. Furthermore, we confirmed and expanded our knowledge on the
447 existence of a protein complex for lipid trafficking between mitochondria and other organelles.
448 In the past, the most abundant plant mitochondrial glycerolipid classes, such as PC, PE, PI, PA, CL,
449 MGDG and DGDG, from *Arabidopsis* cell cultures and calli under phosphate-depleted conditions
450 have been quantified with TLC-GC (Jouhet et al., 2004; Michaud et al., 2016). However, a TLC-
451 GC-based approach lacks the molecular species information concerning acyl chain length and

452 unsaturation degree of the lipids, which are critical parameters to determine the membranes
453 physical properties. In addition, neither sphingolipids nor sterols of mitochondria were profiled
454 to our very best knowledge formerly in *Arabidopsis*.

455 In our study, mitochondria were purified from leaves by differential and Percoll density gradient
456 centrifugations and compared with the well established mitochondrial preparations from
457 suspension cell culture (Jouhet et al., 2004; Klodmann et al., 2011; Behrens et al., 2013;
458 Michaud et al., 2016). Much effort was made to document purity of the resulting organelle
459 fraction: (i) visual inspection of the protein complex composition by 2D BN / SDS PAGE and (ii)
460 label-free quantitative shotgun proteins in combination with SUBAcon evaluation. The SUBAcon
461 database integrates worldwide knowledge on subcellular localization information of Arabidopsis
462 proteins based on *in vitro* or *in vivo* protein targeting experiments, mass spectrometry-based
463 analyses of organellar fractions, protein-protein interaction data and bioinformatics tools for
464 subcellular localization prediction. Based on the latter approach, purity of our mitochondrial
465 fractions can be estimated to be in the range of 90% (87 to 94%, Supplemental Fig. S2). Traces of
466 chloroplasts were present in our fractions. However, even Rubisco, which is considered to be
467 the most abundant chloroplast protein, was detectable only as a very faint spot on the 2D
468 BN/SDS gel of the L-mito fraction (Fig. 1). Finally, quantitative lipid analysis revealed the purity
469 of our mitochondrial fraction. MGDG, DGDG, PG and SQDG are the main components of
470 plastidial membranes (Hölzl and Dörmann, 2019). In *Arabidopsis* chloroplasts, the ratio of
471 MGDG : DGDG : PG : SQDG is about 1:0.5:0.1:0.3 (Awai et al., 2006). In contrast, a distinct ratio
472 of 1:0.3:0.4:0 was detected in L-mito in this study (Fig. 2). Moreover, only a few specific MGDG
473 and DGDG molecular species are enriched in L-mito compared to L-TE (Fig. 3B), suggesting that
474 the cross-contamination from intact plastids or bulk plastidial membranes are insignificant.
475 Interestingly a similar observation was recently made when tagged mitochondria were isolated
476 by affinity purification (Niehaus et al., 2020). However, in previous studies on mitochondria
477 isolated from cell cultures the amount of MGDG was much lower (~1.4 mol % vs. ~15 mol % in
478 Fig. 2) than in the mitochondrial fraction analyzed here from leaves (Jouhet et al., 2004;
479 Michaud et al., 2016). This can only be explained by a higher number of membrane contacts
480 between plastids and mitochondria in leaves as has been observed before in case of phosphate
481 starved cell cultures (Jouhet et al., 2004). On the other hand, more than 85 % of the subunits of

482 the MTL complex (deduced from its composition in yeast mitochondria, Fig. 7) and many OE-
483 localized proteins (Fig. 8) were identified in the mitochondrial samples via our proteomics
484 approach, strongly suggesting that a close contact between mitochondria, the ER and
485 chloroplasts exists in our preparations as has been observed before in *Arabidopsis* cell cultures
486 (Jouhet et al., 2004; Michaud et al., 2016). We conclude that the identified chloroplast lipids and
487 proteins rather originate from small pieces of plastidial membranes and, importantly, the
488 mitochondria-plastid contact sites, which are present in our mitochondrial fraction and
489 contribute to the measured lipid composition. While the protein complexes connecting ER and
490 mitochondria have been well described in yeast, their roles in mediating and/or facilitating lipid
491 translocation are less defined in plants. In contrast to yeast, to our knowledge only one
492 tethering protein has been described in flowering plants up to now (Michaud et al., 2016).

493 With the proteomic and lipidomic datasets as well as the online resources in hand, we assigned
494 central lipid biosynthesis reactions and refined models for a possible exchange of lipid
495 molecules between mitochondria, ER and plastids in plants in Fig. 9. Previous studies in yeast
496 and mammalian cells have shown that mitochondria are capable of synthesizing PE, PA, PG and
497 CL (Flis and Daum, 2013; Horvath and Daum, 2013; Tatsuta et al., 2014). Here, we expand the
498 knowledge that at least the glycerolipids PE and CL can be generated and/or modified in
499 Arabidopsis leaf mitochondria. Considering PE biosynthesis, the rate-limiting enzymes in CDP-
500 ethanolamine and PS decarboxylation pathways, PECT1 and PSD1, respectively, were identified
501 in our mitochondrial samples with higher abundance in C-mito (Fig. 4). It suggests that the
502 generation of mitochondrial PE in the cell culture may be more active in comparison to the
503 leaves. Moreover our observation was supported by earlier studies that localized PECT1 at the
504 mitochondrial periphery and PSD1 in mitochondria in *Arabidopsis* (Mizoi et al., 2006; Nerlich et
505 al., 2007). PE is one of the most abundant glycerophospholipids in biological membranes.
506 Therefore, a high demand is expected to supply mitochondria for their biogenesis in actively
507 dividing cell cultures. The other major component of biological membranes is PC. It is
508 considered to be synthesized in the ER and then transferred through protein complexes
509 connecting ER and mitochondria to mitochondria. The structural information of the enriched
510 lipid species provides evidences for the biosynthesis in the ER as well. Many PE and PC species in
511 mitochondrial samples have longer acyl moieties with 22 to 26 carbons, which can only be

512 synthesized in the ER (Haslam and Kunst, 2013). Conventionally, the majority of PS biosynthesis
513 was assumed to take place in the ER and before being transferred to mitochondria as well. PS
514 and PE, although they are able to interconvert, have distinct lipid profiles from each other,
515 suggesting that only selected lipid species are the substrates of PSD1. In addition, inositol
516 polyphosphate phosphatase 1 (SAL1), which is an enzyme that is involved in phosphoinositide
517 degradation and generates inositol phosphates, was identified in our mitochondrial samples
518 with higher abundance in C-mito comparing to L-mito. This finding confirmed a previous report
519 that localized it in both mitochondria and plastids (Estavillo et al., 2011). Inositol phosphates
520 play crucial roles in many biological processes including gene expression and regulation of cell
521 death through sphingolipids (Alcázar-Román and Wente, 2008; Donahue et al., 2010). Removal
522 of head groups from glycerophospholipids, mostly PC and PE, by phospholipase Dα1 (PLDα1)
523 results in PA, serving as important precursor in other glycerophospholipid biosynthesis
524 pathways (Fig. 9). Comparing to L-TE, the most enriched PA species in L-mito carry 16:0 and 18:0
525 fatty acyl moieties. This corresponds to the enriched PI, PG and DAG species in L-mito,
526 suggesting that PA may serve as an interconverting hinge between these glycerolipids in plant
527 mitochondria. While our study detected PLDα1 preferentially in C-mito samples, previous
528 studies localized it in the cytosol or at the plasmamembrane (Du et al., 2013). This may suggest
529 that PLDα1 localizes to contact sites either between plasmamembrane and mitochondria or
530 between ER and mitochondria. In addition, two glycerol-3-phosphate dehydrogenases were
531 identified (SDP6 and GPDHp). Whereas SDP6 was detected in mitochondria before, GPDHp was
532 localized in the plastid (Nandi et al., 2004; Quettier et al., 2008).

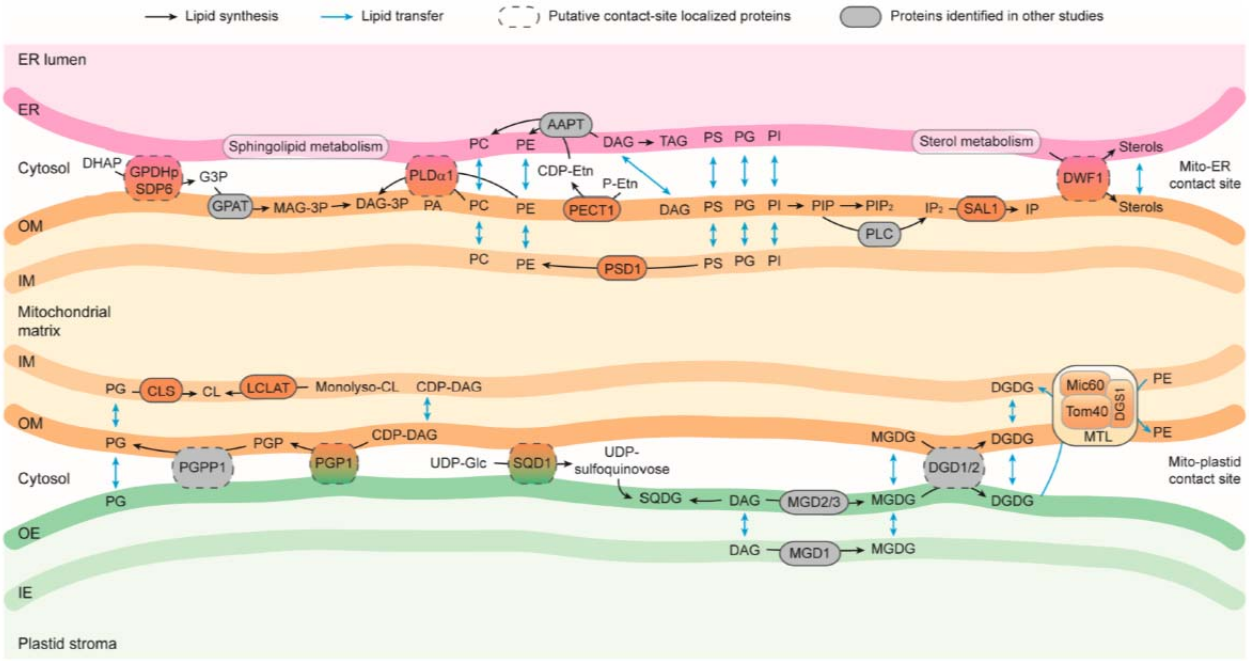


533

534 **Figure 9.** Model of lipid biosynthesis and trafficking within and between mitochondria, ER and
535 plastids in *Arabidopsis*. Lipid synthesis and transfer between membranes are indicated by black
536 and blue arrows, respectively. Proteins identified in L-mito or C-mito with additional ER or
537 plastidic localization based on The Arabidopsis Information Resource (TAIR;
538 www.arabidopsis.org) and the Subcellular localization database for Arabidopsis proteins
539 (SUBAcon; www.suba.live) are considered as putative contact-site localized proteins (dashed
540 frame). Lipid biosynthesis-related proteins indicated in other studies are depicted in grey. Full
541 names and functions of involved proteins are itemized in Supplemental Tab. S1. OM,
542 mitochondrial outer membrane; IM, mitochondrial inner membrane; OE, plastid outer envelope;
543 IE, plastid inner envelope; MTL, mitochondrial transmembrane lipoprotein complex. DHAP,
544 dihydroxyacetone phosphate; G3P, glyceraldehyde 3-phosphate; MAG, monoacylglycerol; DAG,
545 diacylglycerol; Etn, ethanolamine; TAG, triacylglycerol; IP, inositol phosphate; PGP,
546 phosphatidylglycerol phosphate; SQDG, sulfoquinovosyl diacylglycerol.

547

548 An enzyme being involved in synthesizing PG from PA is PGP1. It was found in our proteomic
549 analysis in C-mito samples (Fig. 4). CL can be synthesized through condensation of PG and DAG
550 by CLS, or addition of acyl chains to monolyso-CL by monolysocardiolipin acyltransferase (LCLAT
551 or Tafazzin). All identified enzymes involving in PG and CL biosynthesis, PGP1, CLS and LCLAT,

552 are more abundant in C-mito compared to L-mito. PGP1 was previously found to localize to both
553 mitochondria and plastids (Babiychuk et al., 2003), while CLS was localized to mitochondria
554 (Katayama et al., 2004). This suggests an intensive interaction between mitochondria and
555 plastids in cell cultures because (1) high amounts of proteins localized in contact sites imply a
556 closer connection between the two organelles; (2) more CLS is required to convert the plastid-
557 derived PG which is transferred to mitochondria presumably via membrane contact sites; (3)
558 active energy generation is vital for actively dividing cells and thus a high amount of CL is
559 required to assemble the respiratory chain complexes in mitochondria. This is further supported
560 by the specific PG species found in L-TE. L-TE contains substantial amounts of 16:1 (probably
561 *trans*-$\Delta^3$-16:1)/18:X PG species (~35 mol %) (Fig. 3), which are molecular species synthesized
562 entirely within plastids and probably exclusively localized there (Hölzl and Dörmann, 2019).
563 Therefore, it is very likely that the high amounts of these PG species in L-TE can be attributed to
564 the abundance of plastid membranes particularly thylakoids. Interestingly, the L-mito fraction
565 also contained significant levels (~8 mol %) of 16:1/18:X PG species. These PG species may be
566 not in mitochondria but be derived from the mitochondrion-plastid contact sites or
567 contaminations of plastid membranes (Fig. 9). Nevertheless PG which is directly after its uptake
568 converted into CL in mitochondria (Figs. 2 and 9).

569 Typically, glyceroglycolipids such as MGDG, DGDG and SQDG are considered to be synthesized in
570 plastids and are transferred to other organelles upon stress. For instance, DGDG is transferred
571 from plastidial membranes to other compartments including mitochondrial membranes and the
572 plasma membrane during phosphate starvation to compensate the loss of PC and PE (Jouhet et
573 al., 2004). In addition to vesicular transportation and lipid trafficking via contact sites, emerging
574 evidences support the hypothesis of lipid synthesis in *trans* in yeast and plants (Mehrshahi et al.,
575 2013; Tavassoli et al., 2013; Michaud et al., 2017). That is, enzymes located at one membrane
576 might be capable of catalyzing a reaction on another membrane when in close proximity. In this
577 way, neither tethering proteins nor massive lipid remolding under stress conditions is required,
578 if the mitochondria can acquire lipids without setting up the junctions to other organelles.
579 Therefore, we suspect that the DGDG biosynthesis enzymes, DGD1/2, catalyze the reactions in
580 *trans* or at the mitochondria-plastid contact sites, providing DGDG molecules to compensate the
581 loss of glycerophospholipids in real time (Fig. 4b). In addition, several subunits of the MTL

582 complex were identified in our proteomic approach including Tom40, Mic60, DGS1 etc. (Fig. 7).
583 It establishes a lipid trafficking system removing DGDG from plastids and allocating PE between
584 the IM and OM. Rapid remodeling of the mitochondrial membranes is supported by in *trans*
585 lipid biosynthesis and the MTL complex, likely in close cooperation with other complexes.
586 However, the underlying mechanism of this lipid transportation machinery is still largely
587 unknown. SQDG synthase (SQD1) was identified exclusively in C-mito, but no SQDG molecules
588 were detected (Fig. 4b). Earlier reports localized SQD1 in chloroplasts (Essigmann et al., 1998),
589 suggesting that SQD1 is either co-purified with plastid envelope membranes from cell cultures
590 or is localized in .

591 Sphingolipid biosynthesis takes place at the ER membrane and subsequently in the Golgi
592 apparatus for the addition of carbohydrate residues. Interestingly, in the last decade, several
593 sphingolipid-metabolizing enzymes have been identified in mitochondria purified from yeast
594 and mammalian systems, including Cer synthase and ceramidase (Bionda et al., 2004; Kitagaki et
595 al., 2007; Novgorodov et al., 2011). In animal models, mitochondria-synthesized Cer plays a
596 crucial role in cerebral ischemia-induced mitochondrial dysfunction. The connection between
597 sphingolipids and mitochondria-promoted apoptosis has been proposed in plants as well.
598 Recent studies in *Arabidopsis* have demonstrated that the ratio between LCB-P and Cer is
599 involved in maintaining the balance of cell survival and apoptosis (Watanabe et al., 2013; Bi et
600 al., 2014). However, no sphingolipid biosynthesis enzyme has been identified in plant
601 mitochondria hereto. GIPCs are the most abundant sphingolipids in mitochondria, although still
602 minor comparing to glycerophospholipids. It is known that PM-localized GIPCs are important in
603 signal transduction and intercellular recognition (Lenarčič et al., 2017; Ali et al., 2018). GIPCs
604 may as well establish the communication between mitochondria and other organelles, although
605 further analysis is required to understand the functions of sphingolipids in plant mitochondria.

606 Sterols, although taking part in both biotic and abiotic stress responses, are at low abundance in
607 mitochondrial samples. Sterol biosynthesis primarily takes place in the ER (Schaller, 2003).
608 Among them, sterol C-24 reductase (DWF1) was identified both in L-mito and C-mito, with
609 higher abundance in C-mito. DWF1 has been proposed to mediate the biosynthesis of all
610 phytosterols with higher specificity towards campesterol in Arabidopsis, but this protein was
611 localized to ER membranes (Klahre et al., 1998; Youn et al., 2018). Therefore, we suggest DWF1

612 as an additional contact site localized protein (Fig. 7). High amount of campesterol was detected
613 in L-mito, suggesting the existence of an onsite biosynthesis and/or sterol transporter to
614 facilitate the import of campesterol from the ER. However, unlike mammalian cells wherein
615 cholesterol transport proteins such as steroidogenic acute regulatory protein, StAR (Clark et al.,
616 1995), and MLN64 (Charman et al., 2010) have been identified, little is known about sterol
617 transporters in plants.

618 **Conclusions**

619 In summary, we expanded the knowledge regarding lipid biosynthesis and modification in plant
620 mitochondria by performing a global lipidome analysis of Arabidopsis leaf mitochondria to
621 provide their in-depth lipid molecular species profile including glycerolipids, sphingolipids and
622 sterols. Our proteome data confirmed that PE and CL can be synthesized in these organelles
623 partially by the assistance of putative contact-site localized proteins and / or in *trans* lipid
624 biosynthesis. Based on the proteomic results, we propose and confirm the existence of
625 membrane contact site-localized proteins and their aspects in lipid biosynthesis pathways. This
626 study serves as a foundation for additional researches in unveiling the functional roles of
627 mitochondrial lipids and the mechanisms of mitochondria-dependent signaling pathways.

628

629 **Materials and methods**

630 **Plant materials and growth conditions**

631 Rosette leaves of wild-type *Arabidopsis thaliana* (L.) Heynh Columbia-0 were used for both
632 extracting total lipid extract and purifying mitochondria. After sowing the seeds in pots with
633 three-day cold stratification at 4 °C, seedlings were grown under 16 h-day length at 24 °C with
634 60 % relative humidity and 150 µmol photons $m^{-2}$ $sec^{-1}$ for one week. Young seedlings were
635 transferred to large trays and grown with equal spacing for another three weeks before further
636 experimental procedures.

637 **Suspension culture of *Arabidopsis thaliana***

638 Suspension cultures were established starting from sterilized seeds of *Arabidopsis thaliana* wild-
639 type Columbia-0, grown on MS medium plates containing 0.8 % agar. Plant pieces were
640 transferred to B5 medium agar plates and cultivated for several weeks in the dark for callus
641 induction. Callus was finally transferred into liquid B5 medium including 3 % (w/v) sucrose,
642 0.01 % (w/v) 2,4-dichlorophenoxyacetic acid and 0.001 % (w/v) kinetin. Cultures were incubated
643 on a shaker at 24 °C in the dark. Callus was transferred weekly into new liquid medium (3 g /
644 100 ml).

645 **Mitochondria isolation**

646 *From Arabidopsis rosettes*

647 The mitochondria isolation procedure was described previously (Schikowsky et al., 2018). About
648 200 g of four-week-old *Arabidopsis* rosettes were collected and homogenized at 4 °C with a
649 waring blender in 1 liter disruption buffer (0.3 M sucrose, 60 mM TES, 25 mM tetrasodium
650 pyrophosphate, 10 mM potassium dihydrogen phosphate, 2 mM EDTA, 1 mM glycine, 1 %
651 PVP40, 1 % BSA, 50 mM sodium ascorbate, 20 mM cysteine; pH 8.0) by three times for 10 sec
652 with 30 sec intervals. The following procedures were performed on ice or at 4 °C. Two layers of
653 miracloth with supporting gauze were used to filter the homogenate into a beaker. The
654 remaining plant debris was first grinded with additional sea sand for 10 min by mortar and
655 pestle, and then filtered again through miracloth. The filtrates were combined and centrifuged
656 at 2,500 g for 5 min to eliminate the cell debris. Centrifugation with higher speed at 15,250 g for
657 15 min was applied on the supernatant to pellet mitochondria and other organelles. The
658 resulting pellets were resuspended with a paintbrush in wash buffer (0.3 M sucrose, 10 mM TES,
659 10 mM potassium dihydrogen phosphate; pH 7.5). The samples were adjusted to the final
660 volume of 12 ml with wash buffer and transferred to a Dounce homogenizer. Two strokes of
661 pestle were performed to disrupt large organelles like chloroplasts. Aliquots of 1 ml samples
662 were transferred carefully to Percoll gradients which had been established beforehand by
663 69,400 g centrifugation for 40 min in one-to-one ratio of Percoll and Percoll medium (0.6 M
664 sucrose, 20 mM TES, 2 mM EDTA, 20 mM potassium dihydrogen phosphate, 2 mM glycine;
665 pH 7.5). Mitochondria were separated from other components by centrifuging in the gradients
666 at 17,400 g for 20 min. The resulting mitochondrial fractions formed white clouds at the bottom

667 half of the gradients and were collected by Pasteur pipettes to clean centrifuge tubes. The
668 clean-up procedures were performed three to five times by filling up wash buffer in the
669 centrifuge tubes and pelleting the mitochondria with 17,200 g for 20 min, until the resulting
670 pellet was firm. After each washing steps, two to three pellets were combined in one tube until
671 all mitochondria from one biological replicate were pooled together. The mitochondrial pellets
672 were weighed, resuspended with wash buffer and aliquoted at the concentration of 0.1 g/ml.

673 *From cell cultures*

674 Mitochondria isolation from *Arabidopsis thaliana* suspension cell culture was carried out as
675 described before (Farhat et al., 2019). About 200 g fresh cells were harvested and homogenized
676 using disruption buffer (450 mM sucrose, 15 mM MOPS, 1.5 mM EGTA, 0.6 % (w/v) PVP40, 2 %
677 (w/v) BSA, 10 mM sodium ascorbate, 10 mM cysteine; pH 7.4) and a waring blender. During
678 several washing steps, cell fragments were removed (centrifugation twice for 5 minutes at
679 2,700 g and once for 5 minutes at 8,300 g). Crude mitochondria were pelleted at 17,000 g for
680 10 minutes, resuspended in washing buffer (0.3 M sucrose, 10 mM MOPS, 1 mM EGTA; pH 7.2),
681 homogenized using a Dounce homogenisator and loaded onto discontinuous Percoll gradients
682 (phases of 18 %, 23 % and 40 % Percoll in gradient buffer (0.3 M sucrose, 10 mM MOPS, 0.2 mM
683 EGTA; pH 7.2)). After ultracentrifugation (90 minutes, 70,000 g), purified mitochondria were
684 collected from the 23 %-40 % interphase. For Percoll removal, several washing steps (10 minutes,
685 14,500 g) were performed using resuspension buffer (0.4 M mannitol, 1 mM EGTA, 10 mM
686 tricine; pH 7.2) to gain a firm pellet of purified mitochondria.

687 Each of the three independently purified mitochondria populations from 4-week old rosette
688 leaves (L-mito) and 200 g cell cultures (C-mito), respectively were used for all experiments.

689 **BN/SDS-PAGE**

690 Gel electrophoresis procedures (blue-native (BN) and SDS PAGE) were performed as described
691 previously (Senkler et al., 2018), based on the published protocol given in (Wittig et al., 2006).

692 **Label-free quantitative shotgun proteomics**

693 *Protein sample preparation*

694 Sample preparation for shotgun proteome analysis was performed as described before (Thal et
695 al., 2018). The protein content of the mitochondrial fractions was determined using a Bradford
696 assay kit (Thermo Scientific, Rockford, USA). 50 µg protein of each sample were loaded onto a
697 SDS gel for sample purification (Thal et al., 2018). Electrophoresis was stopped when the
698 proteins reached the border between the stacking and the separating gel. Gels were
699 subsequently incubated in fixation solution (15% (v.v) ethanol; 10% (v.v) acetic acid) for 30 min,
700 stained for 1 h with Coomassie Brilliant Blue G250, and finally the protein band at the border of
701 the two gel phases was cut out into cubes with edge lengths of approximately 1 mm.
702 Trypsination of the proteins was carried out as described previously (Fromm et al., 2016).

703 *Shotgun proteomic LC-MS analysis*

704 Label-free quantitative mass spectrometric analyses of whole mitochondrial protein samples
705 from cell culture and long day *Arabidopsis thaliana* leaves were performed as outlined before
706 (Thal et al., 2018) using an Ultimate 3000 UPLC coupled to a Q Exactive Orbitrap mass
707 spectrometer (Thermo Scientific, Dreieich, Germany).

708 *Data processing*

709 In a first step, the resulting MS data were processed using the Proteome Discoverer Software
710 (Thermo Fisher Scientific, Dreieich, Germany) and searched with the Mascot search engine
711 (www.matrixscience.com) against the tair10 protein database (downloaded from
712 www.arabidopsis.org). For quantitative analyses, MS data were further processed as outlined
713 before (Rugen et al., 2019) using the MaxQuant software package (version 1.6.4.0), the
714 Andromeda search engine (Cox and Mann, 2008) and the tair10 protein database. For
715 determination of sample purity, peptide intensities were used, combined with the subcellular
716 locations of assigned proteins as given by SUBAcon from the SUBA platform (www.suba.live)
717 (Hooper et al., 2017). A proteomic heatmap was generated using the NOVA software
718 (www.bioinformatik.uni-frankfurt.de/tools/nova/index.php)(Giese et al., 2015). Identified
719 proteins of all six datasets (three biological replicates of leaf total mitochondrial protein (L-mito
720 1,2,3) and cell culture total mitochondrial protein (C-mito 1,2,3)) were hierarchically clustered in
721 a heatmap based on iBAQ (intensity Based Absolute Quantification) values (for primary results
722 see Supplemental Tab. S1).

723 **Lipid extraction**

724 Total lipid extract from leaf (L-TE) was obtained as described (Tarazona et al., 2015). Briefly,
725 mixture of 150 mg frozen leaf powder or 100 mg mitochondria and 6 ml extraction buffer
726 (propan-2-ol : hexane : water, 60:26:14 (v.v.v)) was incubated at 60 °C with shaking for 30 min.
727 After centrifugation at 800 g for 20 min, the clear supernatant was transferred to clean tubes
728 and evaporated under stream of nitrogen gas until dryness. Samples were reconstituted in
729 800 µl of TMW (tetrahydrofuran (THF) : methanol : water, 4:4:1 (v.v.v)). Procedure for extracting
730 the mitochondrial lipids was adjusted by substituting the water fraction of the extraction buffer
731 by equal volume of the mitochondrial aliquot. Further process was continued as described
732 above.

733 **Lipid quantification**

734 *TLC separation of lipid classes*

735 Lipid extracts from 500 mg mitochondria and 50 mg leaves were spotted onto TLC 60 plates (20
736 × 20 $cm^2$, Merck KGaA, Darmstadt, Germany) in parallel with the following standards: PC
737 (Larodan, Solna, Sweden), PE, CL, and PG (Avanti Polar Lipids, Birmingham, AL, USA), MGDG, and
738 DGDG (purified from plant lipid extracts). Extracts were developed by a solvent mixture of
739 chloroform : methanol : acetic acid (65:25:8 (v.v.v)). After visualizing the lipid spots under
740 528 nm UV light, the bands were scrapped out and converted to fatty acid methyl esters (FAME)
741 before GC/FID analysis.

742 *Acidic transesterification*

743 Glycerolipids were transesterified by acidic methanolysis (Miquel and Browse, 1992) and
744 converted to fatty acid methyl esters (FAME). The lipid-bound silica powder from corresponding
745 spots on the TLC plate were scrapped out and added to 1 ml FAME solution (methanol : toluene :
746 sulfuric acid : dimethoxypropane, 33:17:1.4:1 (v.v.v.v)) with 5 µg tripentadecanoin as an internal
747 standard. After 1 h incubation at 80 °C, 1.5 ml saturated NaCl solution and 1.2 ml hexane were
748 added subsequently. The resulting FAME was collected from the hexane phase, dried, and
749 reconstituted in 10 µl acetonitrile.

750 *GC/FID analysis*

751 Lipid-bound fatty acids were analyzed after converting to FAMEs by a 6890N Network GC/FID
752 System with a medium polar cyanopropyl DB-23 column (30 m × 250 µm × 25 nm; Agilent
753 Technologies, Waldbronn, Germany) using helium as the carrier gas at 1 ml $min^{-1}$. Samples were
754 injected at 220 °C with an Agilent 7683 Series injector in split mode. After 1 min at 150 °C, the
755 oven temperature raised to 200 °C at the rate of 8 °C $min^{-1}$, increased to 250 °C in 2 min, and
756 held at 250 °C for 6 min. Peak integration was performed using the GC ChemStation (Agilent
757 Technologies).

758 **Lipid derivatization**

759 Phosphate-containing lipids - phosphatidic acids (PA), phosphoinositides (PIPs) and long-chain
760 base phosphates (LCB-P) - were derivatized to enhance their chromatographic separation and
761 mass spectrometric detection. Methylation procedure was applied on PA and PIPs as followed.
762 Aliquots of 100 µl lipid extracts were first brought to dryness under stream of nitrogen gas and
763 reconstituted with 200 µl methanol. Methylation reaction took place after the supply of 3.3 µl
764 trimethylsilyldiazomethane. After 30 min incubation at room temperature, the reaction was
765 terminated by neutralizing with 1 µl of 1.7 M acetic acid. Samples were dried under nitrogen gas
766 and redissolved in 100 µl TMW. Acetylation procedure was applied on LCB-P. Aliquots of 100 µl
767 lipid extracts were brought to dryness and reconstituted with 100 µl pyridine and 50 µl acetic
768 anhydride. After 30 min incubation at 50 °C, samples were dried under stream of nitrogen gas
769 with 50 °C water bath. To redissolve the samples, 100 µl TMW was used as the final solvent to
770 proceed with lipid analysis.

771 **Global lipidomic analysis with LC-MS**

772 Analysis conditions and system setup were as described (Tarazona et al., 2015). Samples were
773 separated by an ACQUITY UPLC system (Waters Crop., Milford, MA, USA) with a HSS T3 column
774 (100 mm x 1 mm, 1.8 µl; Waters Crop.), ionized by a chip-based nanoelectrospray using TriVersa
775 Nanomate (Advion BioScience, Ithaca, NY, USA) and analyzed by a 6500 QTRAP tandem mass
776 spectrometer (AB Sciex, Framingham, MA, USA). Aliquots of 2 µl were injected and separated
777 with a flow rate of 0.1 ml $min^{-1}$. The solvent system composed of methanol : 20 mM ammonium
778 acetate (3:7 (v.v)) with 0.1 % (v.v) acetic acid (solvent A) and THF : methanol : 20 mM
779 ammonium acetate (6:3:1 (v.v.v)) with 0.1 % (v.v) acetic acid (solvent B). According to the lipid

780 classes, different linear gradients were applied: start from 40 %, 65 %, 80 % or 90 % B for 2 min;
781 increase to 100 % B in 8 min; hold for 2 min and re-equilibrate to the initial conditions in 4 min.
782 Starting condition of 40 % solvent B were utilized for long-chain bases (LCB) and phosphorylated
783 long-chain bases (LCB-P); 80 % for diacylglycerol (DAG); 90 % for steryl esters (SE); 65 % for the
784 remaining lipid classes. Retention time alignment and peak integration were performed with
785 MultiQuant (AB Sciex). Quantitative results were calculated according to the amount of internal
786 standards.

787 **Biosynthesis pathways construction**

788 The Arabidopsis Information Resource (TAIR; www.arabidopsis.org), the Subcellular localization
789 database for Arabidopsis proteins (SUBAcon; www.suba.live), Kyoto Encyclopedia of Genes and
790 Genomes (KEGG; www.genome.jp/kegg) and the shotgun proteomic analyses of L-mito and C-
791 mito were combined to construct the lipid biosynthesis pathways in plant mitochondria.
792 Additionally, lipidomics data are depicted in the pathways to illustrate the biosynthetic fluxes.

793

794 **Supplemental Data**

795 **Supplemental Figure S1.** Purity inspection of mitochondrial protein complexes and
796 supercomplexes by two-dimensional blue-native/SDS PAGE. Mitochondrial fractions isolated
797 from Arabidopsis leaves (L-mito 1 and L-mito 3) and from Arabidopsis cell cultures (C-mito1 and
798 C-mito 3) were separated by 2D PAGE and Coomassie-stained (corresponding gels of fractions L-
799 mito 2 and C-mito 2 see Fig. 1). Numbers on top and to the left of the 2D gels refer to the
800 masses of standard protein complexes / proteins (in kDa), the roman numbers above the gels to
801 the identity of OXPHOS complexes (see Fig. 1 for detailed information). The arrows indicate the
802 large (L; 53,5 kDa) and the small (S; 14.5 kDa) subunit of Rubisco. To further confirm the
803 reproducibility of the preparations, 2D blue-native/SDS reference gels for mitochondrial and
804 chloroplast fractions (Mito-ref, Cp-ref) from *A. thaliana* are given to the bottom of the figure
805 (gels were taken from (Klodmann et al., 2011) and (Behrens et al., 2013)). Identity of the protein
806 complexes visible on the chloroplast reference gel: PSI – photosystem I; PSII – photosystem II;
807 Rub – Rubisco; LHCII – light harvesting complex II.

808 **Supplemental Figure S2.** Purity of mitochondrial fractions as determined by label-free quantitative
809 shot gun proteomics. Three mitochondrial fractions isolated from Arabidopsis leaves (L-mitos) and cell
810 cultures (C-mitos) were analysed. Summed-up peptide intensities were calculated for subcellular
811 compartments based on protein assignments as given by SUBAcon (The Subcellular localization database
812 for Arabidopsis proteins; www.suba.live**).** Blue: mitochondria; green: plastids; gray: others; numbers in %.

813 **Supplemental Figure S3.** Fatty acid profiles of the glycerolipids from L-mito, L-TE, C-mito and C-TE.
814 Heat maps illustrate the difference of the fatty acid distribution based on LC-MS/MS analyses. The heat
815 map colors represent mean intensity values according to the color map on the low right-hand side. Each
816 column represents one lipid class wherein the acyl moieties of all species are listed and summarized to
817 100 %. Data represent mean values in mol % from three independent experiments which were also used
818 for proteomics (Supplemental Tab. S1).

819 **Supplemental Figure S4.** Workflow for the construction of the biosynthesis pathways. Multiple
820 databases were combined to build the lipid biosynthesis pathways in mitochondria, The Arabidopsis
821 Information Resource (TAIR; www.arabidopsis.org), the Subcellular localization database for Arabidopsis
822 proteins (SUBAcon; www.suba.live), Kyoto Encyclopedia of Genes and Genomes (KEGG;
823 www.genome.jp/kegg) and the proteomic datasets of isolated mitochondria in this study. Information of
824 protein localizations and backbones of the biosynthesis pathways were obtained from TAIR, SUBAcon
825 and KEGG, respectively.

826 **Supplemental Figure S5.** Additional lipid biosynthesis enzymes which do not match with analyzed lipid
827 classes in this study. Enzymes of (a) fatty acid biosynthesis, (b) unsaturated fatty acid biosynthesis, (c)
828 lipoic acid metabolism and (d) ubiquinone and other terpenoid-quinone biosynthesis illustrate the
829 general lipid biosynthesis in Arabidopsis mitochondria. Heat maps visualize the protein abundance based
830 on shotgun proteomic analyses of three independent experiments of purified mitochondria from leaves
831 and cell culture. The heat map colors represent mean intensity values according to the color map on the
832 low right-hand side. Blue: proteins identified in the proteomic analysis of this study and also predicted to
833 localize in mitochondria; green: proteins identified in the proteomic analysis of this study but predicted
834 to localize in other organelles; bold font: exclusively localized in mitochondria; italic font: only identified
835 in one of the mitochondrial populations. Further full names and functions are itemized in Supplemental
836 Tab. S3. In the heat maps, proteins with high and low abundance are depicted in yellow and black,
837 respectively. Predicted protein localization was based on The Arabidopsis Information Resource (TAIR;
838 www.arabidopsis.org) and the Subcellular localization database for Arabidopsis proteins (SUBAcon;
839 www.suba.live).

840 **Supplemental Table S1.** Overall proteins identified in the proteomic approach.

841 **Supplemental Table S2.** Overall lipids identified in the lipidomic approach.

842 **Supplemental Table S3.** Lipid biosynthesis-related proteins identified in the proteomic approach.

843 **Supplemental Table S4.** List of subunits of the MTL identified in the proteomic approach.

844 **Supplemental Table S5.** Proteins assigned to plastids regarding to SUBAcon.

845

846 **Acknowledgements**

847 We are grateful for the technical assistance from Sabine Freitag. YL has been a doctoral student
848 of the Ph.D. program "Molecular Biology" – International Max Planck Research School and the
849 Göttingen Graduate School for Neurosciences, Biophysics, and Molecular Biosciences (GGNB)
850 (DFG grant GSC 226) at the Georg August University Göttingen.

851 **Funding information**

852 IF and HPB acknowledge funding through the German Research Foundation (DFG: INST 186/822-
853 1, INST 186/1167-1, INST 187/503-1 and ZUK 45/2010).

854

855

856 **References**

857 **Achleitner G, Gaigg B, Krasser A, Kainersdorfer E, Kohlwein SD, Perktold A, Zellnig G, Daum G** (1999)
858 Association between the endoplasmic reticulum and mitochondria of yeast facilitates interorganelle
859 transport of phospholipids through membrane contact. Eur J Biochem **264:** 545-553

860 **Alcázar-Román AR, Wente SR** (2008) Inositol polyphosphates: a new frontier for regulating gene
861 expression. Chromosoma **117:** 1-13

862 **Ali U, Li H, Wang X, Guo L** (2018) Emerging roles of sphingolipid signaling in plant response to biotic and
863 abiotic stresses. Mol Plant **11:** 1328-1343

864 **Awai K, Xu C, Tamot B, Benning C** (2006) A phosphatidic acid-binding protein of the chloroplast inner
865 envelope membrane involved in lipid trafficking. Proc Natl Acad Sci USA **103:** 10817-10822

866 **Babiychuk E, Müller F, Eubel H, Braun H-P, Frentzen M, Kushnir S** (2003) *Arabidopsis*
867 phosphatidylglycerophosphate synthase 1 is essential for chloroplast differentiation, but is
868 dispensable for mitochondrial function. Plant J **33:** 899 - 909
869 **Behrens C, Blume C, Senkler M, Eubel H, Peterhänsel C, Braun H-P** (2013) The 'protein complex
870 proteome' of chloroplasts in *Arabidopsis thaliana*. Journal of Proteomics **91:** 73-83
871 **Bi F-C, Liu Z, Wu J-X, Liang H, Xi X-L, Fang C, Sun T-J, Yin J, Dai G-Y, Rong C, Greenberg JT, Su W-W, Yao**
872 **N** (2014) Loss of ceramide kinase in *Arabidopsis* impairs defenses and promotes ceramide
873 accumulation and mitochondrial $H_2O_2$ bursts. Plant Cell **26:** 3449-3467
874 **Bionda C, Portoukalian J, Schmitt D, Rodriguez-Lafrasse C, Ardail D** (2004) Subcellular
875 compartmentalization of ceramide metabolism: MAM (mitochondria-associated membrane) and/or
876 mitochondria? Biochem J **382:** 527-533
877 **Birner R, Burgermeister M, Schneiter R, Daum G** (2001) Roles of phosphatidylethanolamine and of its
878 several biosynthetic pathways in *Saccharomyces cerevisiae*. Molecular Biology of the Cell **12:** 997-
879 1007.
880 **Bligny R, Douce R** (1980) A precise localization of cardiolipin in plant cells. Biochim Biophys Acta **617:**
881 254-263
882 **Braun H-P** (2020) The Oxidative phosphorylation system of the mitochondria in plants. Mitochondrion **53:**
883 66-75
884 **Cacas J-L, Furt F, Le Guédard M, Schmitter J-M, Buré C, Gerbeau-Pissot P, Moreau P, Bessoule J-J,**
885 **Simon-Plas F, Mongrand S** (2012) Lipids of plant membrane rafts. Prog Lipid Res **51:** 272-299
886 **Charman M, Kennedy BE, Osborne N, Karten B** (2010) MLN64 mediates egress of cholesterol from
887 endosomes to mitochondria in the absence of functional Niemann-Pick Type C1 protein. J Lipid Res
888 **51:** 1023-1034
889 **Clark BJ, Pezzi V, Stocco DM, Rainey WE** (1995) The steroidogenic acute regulatory protein is induced by
890 angiotensin II and $K^+$ in H295R adrenocortical cells. Molecular and Cellular Endocrinology **115:** 215-
891 219
892 **Cox J, Mann M** (2008) MaxQuant enables high peptide identification rates, individualized p.p.b.-range
893 mass accuracies and proteome-wide protein quantification. Nature Biotechnol **26:** 1367-1372
894 **Donahue JL, Alford SR, Torabinejad J, Kerwin RE, Nourbakhsh A, Ray WK, Hernick M, Huang X, Lyons**
895 **BM, Hein PP, Gillaspy GE** (2010) The *Arabidopsis thaliana myo*-inositol 1-phosphate synthase1 gene
896 is required for *myo*-inositol synthesis and suppression of cell death. Plant Cell **22:** 888-903
897 **Douce R, Mannella CA, Bonner WD** (1972) Site of the biosynthesis of CDP-diglyceride in plant
898 mitochondria. Biochem Biophys Res Commun **49:** 1504-1509

899 **Du Z-Y, Chen M-X, Chen Q-F, Xiao S, Chye M-L** (2013) Arabidopsis acyl-CoA-binding protein ACBP1
900 participates in the regulation of seed germination and seedling development. Plant J **74:** 294-309
901 **Essigmann B, Guler S, Narang RA, Linke D, Benning C** (1998) Phosphate availability affects the thylakoid
902 lipid composition and the expression of *SQD1*, a gene required for sulfolipid biosynthesis in
903 *Arabidopsis thaliana*. Proc Natl Acad Sci USA **95:** 1950-1955
904 **Estavillo GM, Crisp PA, Pornsiriwong W, Wirtz M, Collinge D, Carrie C, Giraud E, Whelan J, David P,**
905 **Javot H, Brearley C, Hell R, Marin E, Pogson BJ** (2011) Evidence for a SAL1-PAP chloroplast
906 retrograde pathway that functions in drought and high light signaling in *Arabidopsis* Plant Cell **23:**
907 3992-4012
908 **Farhat N, Hichri S, Hildebrandt TM, Debez A, Braun H-P** (2019) Composition and stability of the oxidative
909 phosphorylation system in the halophile plant *Cakile Maritima*. Front Plant Sci **10:** 1010
910 **Flis VV, Daum G** (2013) Lipid transport between the endoplasmic reticulum and mitochondria. Cold
911 Spring Harbor Perspectives in Biology **5:** a013235
912 **Fromm S, Senkler J, Eubel H, Peterhänsel C, Braun H-P** (2016) Life without complex I: proteome analyses
913 of an Arabidopsis mutant lacking the mitochondrial NADH dehydrogenase complex. J Exp Bot **67:**
914 3079-3093
915 **Giese H, Ackermann Jr, Heide H, Bleier L, DrÃ¶se S, Wittig I, Brandt U, Koch I** (2015) NOVA: a software
916 to analyze complexome profiling data. Bioinformatics **31:** 440-441
917 **Gray MW, Burger G, Lang BF** (1999) Mitochondrial evolution. Science **283:** 1476-1481
918 **Haslam TM, Feussner I** (2022) Diversity in sphingolipid metabolism across land plants. J Exp Bot **73:**
919 2785-2798
920 **Haslam TM, Kunst L** (2013) Extending the story of very-long-chain fatty acid elongation. Plant Sci **210:** 93-
921 107
922 **Heilmann I** (2016) Phosphoinositide signaling in plant development. Development **143:** 2044-2055
923 **Hölzl G, Dörmann P** (2019) Chloroplast Lipids and Their Biosynthesis. Annu Rev Plant Biol **70:** null
924 **Hölzl G, Dörmann P** (2019) Chloroplast lipids and their biosynthesis. Annu Rev Plant Biol **70:** 51-81
925 **Hooper CM, Castleden IR, Tanz SK, Aryamanesh N, Millar AH** (2017) SUBA4: the interactive data analysis
926 centre for Arabidopsis subcellular protein locations. Nucleic Acids Res **45:** D1064-D1074
927 **Horvath SE, Daum G** (2013) Lipids of Mitochondria. Prog Lipid Res **52:** 590-614
928 **Inoue K** (2007) The chloroplast outer envelope membrane: the edge of light and excitement. Journal of
929 Integrative Plant Biology **49:** 1100-1111
930 **Inoue K** (2011) Emerging roles of the chloroplast outer envelope membrane. Trends Plant Sci **16:** 550-
931 557

932 **Jacoby RP, Li L, Huang S, Pong Lee C, Millar AH, Taylor NL** (2012) Mitochondrial composition, function
933 and stress response in plants. Journal of Integrative Plant Biology **54:** 887-906
934 **Jouhet J, Marechal E, Baldan B, Bligny R, Joyard J, Block MA** (2004) Phosphate deprivation induces
935 transfer of DGDG galactolipid from chloroplast to mitochondria. Journal of Cell Biology **167:** 863-874
936 **Katayama K, Sakurai I, Wada H** (2004) Identification of an *Arabidopsis thaliana* gene for cardiolipin
937 synthase located in mitochondria. FEBS Lett **577:** 193-198
938 **Kim J, Na YJ, Park SJ, Baek S-H, Kim DH** (2019) Biogenesis of chloroplast outer envelope membrane
939 proteins. Plant Cell Rep **38:** 783-792
940 **Kitagaki H, Cowart LA, Matmati N, Vaena de Avalos S, Novgorodov SA, Zeidan YH, Bielawski J, Obeid**
941 **LM, Hannun YA** (2007) Isc1 regulates sphingolipid metabolism in yeast mitochondria. Biochim
942 Biophys Acta **1768:** 2849-2861
943 **Klahre U, Noguchi T, Fujioka S, Takatsuto S, Yokota T, Nomura T, Yoshida S, Chua NH** (1998) The
944 Arabidopsis *DIMINUTO/DWARF1* gene encodes a protein involved in steroid synthesis. Plant Cell **10:**
945 1677-1690
946 **Klodmann J, Senkler M, Rode C, Braun H-P** (2011) Defining the *protein complex proteome* of plant
947 mitochondria. Plant Physiol **157:** 587-598
948 **Lenarčič T, Albert I, Böhm H, Hodnik V, Pirc K, Zavec AB, Podobnik M, Pahovnik D, Žagar E, Pruitt R,**
949 **Greimel P, Yamaji-Hasegawa A, Kobayashi T, Zienkiewicz A, Gömann J, Mortimer JC, Fang L,**
950 **Mamode-Cassim A, Deleu M, Lins L, Oecking C, Feussner I, Mongrand S, Anderluh G, Nürnberger T**
951 (2017) Eudicot plant-specific sphingolipids determine host selectivity of microbial NLP cytolysins.
952 Science **358:** 1431-1434
953 **Li-Beisson Y, Shorrosh B, Beisson F, Andersson MX, Arondel V, Bates PD, Baud S, Bird D, DeBono A,**
954 **Durrett TP, Franke RB, Graham IA, Katayama K, Kelly AA, Larson T, Markham JE, Miquel M, Molina**
955 **I, Nishida I, Rowland O, Samuels L, Schmid KM, Wada H, Welti R, Xu C, Zallot R, Ohlrogge J** (2013)
956 Acyl-lipid metabolism. *In* C Somerville, E Meyerowitz, eds, The Arabidopsis Book. The American
957 Society of Plant Biologists, Rockville, MD, USA, p e0161
958 **Li L, Lavell A, Meng X, Berkowitz O, Selinski J, van de Meene A, Carrie C, Benning C, Whelan J, De Clercq**
959 **I, Wang Y** (2019) Arabidopsis DGD1 SUPPRESSOR1 is a subunit of the mitochondrial contact site and
960 cristae organizing system and affects mitochondrial biogenesis. Plant Cell **31:** 1856-1878
961 **Liebisch G, Fahy E, Aoki J, Dennis EA, Durand T, Ejsing C, Fedorova M, Feussner I, Griffiths WJ, Koefeler**
962 **H, Merrill AH, Murphy RC, O'Donnell VB, Oskolkova OV, Subramaniam S, Wakelam M, Spener F**
963 (2020) Update on LIPID MAPS classification, nomenclature and shorthand notation for MS-derived
964 lipid structures. J Lipid Res **61:** 1539–1555

965 **Mehrshahi P, Stefano G, Andaloro JM, Brandizzi F, Froehlich JE, DellaPenna D** (2013) Transorganellar
966 complementation redefines the biochemical continuity of endoplasmic reticulum and chloroplasts.
967 Proc Natl Acad Sci USA **110:** 12126-12131
968 **Michaud M, Gros V, Tardif M, Brugiere S, Ferro M, Prinz WA, Toulmay A, Mathur J, Wozny M, Falconet**
969 **D, Marechal E, Block MA, Jouhet J** (2016) AtMic60 is involved in plant mitochondria lipid trafficking
970 and is part of a large complex. Curr Biol **26:** 627-639
971 **Michaud M, Prinz WA, Jouhet J** (2017) Glycerolipid synthesis and lipid trafficking in plant mitochondria.
972 The FEBS Journal **284:** 376-390
973 **Miquel M, Browse J** (1992) *Arabidopsis* mutants deficient in polyunsaturated fatty acid synthesis. J Biol
974 Chem **267:** 1502-1509
975 **Mizoi J, Nakamura M, Nishida I** (2006) Defects in CTP:PHOSPHORYLETHANOLAMINE
976 CYTIDYLYLTRANSFERASE affect embryonic and postembryonic development in *Arabidopsis*. Plant
977 Cell **18:** 3370-3385
978 **Moreau F, Dupont J, Lance C** (1974) Phospholipid and fatty acid composition of outer and inner
979 membranes of plant mitochondria. Biochim Biophys Acta **345:** 294-304
980 **Morré DJ, Merritt WD, Lembi CA** (1971) Connections between mitochondria and endoplasmic reticulum
981 in rat liver and onion stem. Protoplasma **73:** 43-49
982 **Müller F, Frentzen M** (2001) Phosphatidylglycerophosphate synthases from *Arabidopsis thaliana*. FEBS
983 Lett **509:** 298-302
984 **Nandi A, Welti R, Shah J** (2004) The *Arabidopsis thaliana* dihydroxyacetone phosphate reductase gene
985 *SUPPRESSOR OF FATTY ACID DESATURASE DEFICIENCY1* is required for glycerolipid metabolism and
986 for the activation of systemic acquired resistance. Plant Cell **16:** 465–477
987 **Nerlich A, von Orlow M, Rontein D, Hanson AD, Dörmann P** (2007) Deficiency in phosphatidylserine
988 decarboxylase activity in the *psd*1 *psd*2 *psd*3 triple mutant of Arabidopsis affects
989 phosphatidylethanolamine accumulation in mitochondria. Plant Physiol **144:** 904-914
990 **Niehaus M, Straube H, Künzler P, Rugen N, Hegermann J, Giavalisco P, Eubel H, Witte C-P, Herde M**
991 (2020) Rapid affinity purification of tagged plant mitochondria (Mito-AP) for metabolome and
992 proteome analyses. Plant Physiol **182:** 1194–1210
993 **Novgorodov SA, Wu BX, Gudz TI, Bielawski J, Ovchinnikova TV, Hannun YA, Obeid LM** (2011) Novel
994 pathway of ceramide production in mitochondria. J Biol Chem **286:** 25352-25362
995 **Quettier A-L, Shaw E, Eastmond PJ** (2008) SUGAR-DEPENDENT6 Encodes a Mitochondrial Flavin Adenine
996 Dinucleotide-Dependent Glycerol-3-P Dehydrogenase, Which Is Required for Glycerol Catabolism
997 and Postgerminative Seedling Growth in Arabidopsis. Plant Physiol **148:** 519-528

998 **Rugen N, Straube H, Franken LE, Braun H-P, Eubel H** (2019) Complexome profiling reveals association of
999 PPR proteins with ribosomes in the mitochondria of plants. Molecular & Cellular Proteomics **18:**
1000 1345-1362
1001 **Schaller H** (2003) The role of sterols in plant growth and development. Prog Lipid Res **42:** 163-175
1002 **Schikowsky C, Thal B, Braun H-P, Eubel H** (2018) Sample preparation for analysis of the plant
1003 mitochondrial membrane proteome. *In* H-P Mock, A Matros, K Witzel, eds, Plant Membrane
1004 Proteomics: Methods and Protocols. Springer New York, New York, NY, pp 163-183
1005 **Senkler J, Rugen N, Eubel H, Hegermann J, Braun H-P** (2018) Absence of complex I implicates
1006 rearrangement of the respiratory chain in european mistletoe. Curr Biol **28:** 1606-1613.e1604
1007 **Simm S, Papasotiriou D, Ibrahim M, Leisegang M, Müller B, Schorge T, Karas M, Mirus O, Sommer M,**
1008 **Schleiff E** (2013) Defining the core proteome of the chloroplast envelope membranes. Front Plant
1009 Sci **4**
1010 **Staehelin LA** (1997) The plant ER: a dynamic organelle composed of a large number of discrete functional
1011 domains. Plant J **11:** 1151-1165
1012 **Tarazona P, Feussner K, Feussner I** (2015) An enhanced plant lipidomics method based on multiplexed
1013 liquid chromatography–mass spectrometry reveals additional insights into cold- and drought-
1014 induced membrane remodeling. Plant J **84:** 621-633
1015 **Tatsuta T, Scharwey M, Langer T** (2014) Mitochondrial lipid trafficking. Trends Cell Biol **24:** 44-52
1016 **Tavassoli S, Chao JT, Young BP, Cox RC, Prinz WA, de Kroon AIPM, Loewen CJR** (2013) Plasma
1017 membrane - endoplasmic reticulum contact sites regulate phosphatidylcholine synthesis. EMBO rep
1018 **14:** 434-440
1019 **Thal B, Braun H-P, Eubel H** (2018) Proteomic analysis dissects the impact of nodulation and biological
1020 nitrogen fixation on *Vicia faba* root nodule physiology. Plant Mol Biol **97:** 233-251
1021 **Vance JE** (1990) Phospholipid synthesis in a membrane fraction associated with mitochondria. J Biol
1022 Chem **265:** 7248-7256
1023 **Watanabe M, Balazadeh S, Tohge T, Erban A, Giavalisco P, Kopka J, Mueller-Roeber B, Fernie AR,**
1024 **Hoefgen R** (2013) Comprehensive Dissection of Spatiotemporal Metabolic Shifts in Primary,
1025 Secondary, and Lipid Metabolism during Developmental Senescence in Arabidopsis. Plant Physiol
1026 **162:** 1290-1310
1027 **Wittig I, Braun H-P, Schägger H** (2006) Blue native PAGE. Nat Protoc **1:** 418-428
1028 **Xu C, Hartel H, Wada H, Hagio M, Yu B, Eakin C, Benning C** (2002) The *pgp1* mutant locus of Arabidopsis
1029 encodes a phosphatidylglycerolphosphate synthase with impaired activity. Plant Physiol **129:** 594-
1030 604

1031 **Xu Y, Malhotra A, Ren M, Schlame M** (2006) The enzymatic function of Tafazzin. J Biol Chem **281:** 39217-
1032 39224
1033 **Yamaoka Y, Yu Y, Mizoi J, Fujiki Y, Saito K, Nishijima M, Lee Y, Nishida I** (2011) *PHOSPHATIDYLSERINE*
1034 *SYNTHASE1* is required for microspore development in *Arabidopsis thaliana*. Plant J **67:** 648-661
1035 **Youn JH, Kim T-W, Joo S-H, Son S-H, Roh J, Kim S, Kim T-W, Kim S-K** (2018) Function and molecular
1036 regulation of DWARF1 as a C-24 reductase in brassinosteroid biosynthesis in Arabidopsis. J Exp Bot
1037 **69:** 1873-1886